



UNICO I+D Project
Grant No. 6G-INTEGRATION-4

Environmental control system energy load definition

Abstract

This report presents a design method for the thermal system of stratospheric airships, considering the thermal and power effects of solar array and hydrogen. The thermal performance of a stratospheric airship with photovoltaic array is also simulated and analysed. The results show that solar radiation has a significant impact on the temperature and flow of the airship, and that the design method can reduce the temperature difference of the solar array and increase the payload mass.

Document properties

Document number	E10_6G-INTEGRATION-4_EDT
Document title	Environmental control system energy load definition
Document responsible	Eduardo Cano Corral (Edair Technologies)
Document editor	Raul Herrero Moreno (Edair Technologies)
Editorial team	Pedro Baquero Jaen (Edair Technologies)
Target dissemination level	Public
Status of the document	Final
Version	1.0

Production properties

Reviewers	Eduardo Arca Ramirez (Edair Technologies) Daniel Segovia Vargas (UC3M)
------------------	---

Document history

Revision	Date	Issued by	Description
1.0	29/11/2023	Raul Herrero Moreno	Initial

Disclaimer

This document has been produced in the context of the 6G-INTEGRATION-4 Project. The research leading to these results has received funding from the Name Programme under grant agreement 6G-INTEGRATION-4.

All information in this document is provided "as is" and no guarantee or warranty is given that the information is fit for any particular purpose. The user thereof uses the information at its sole risk and liability.

For the avoidance of all doubts, the Name has no liability in respect of this document, which is merely representing the author's view.

Contents

List of Figures.....	5
List of Tables.....	6
List of Acronyms	7
Executive Summary.....	9
1. Introduction.....	10
2. Thermal Control.....	11
2.1. State-of-the-Art – Passive Systems.....	13
2.1.1. Paints, Coatings, and Tapes	15
2.1.2. Multi-layer Insulation	16
2.1.3. Thermal Straps.....	17
2.1.4. Thermal Contact Conductance and Bolted Joint Conductance.....	19
2.1.5. Thermal Interface Materials and Conductive Gaskets	19
2.1.6. Sunshields.....	20
2.1.7. Thermal Louvers.....	21
2.1.8. Deployable Radiators.....	21
2.1.9. Heat Pipes.....	23
2.1.10. Phase Change Materials/ Thermal Storage Units	25
2.1.11. Thermal Switches.....	26
2.1.12. Multifunctional Thermal Structures.....	26
2.2. State-of-the-Art – Active Systems.....	26
2.2.1. Heaters.....	27
2.2.2. Cryocoolers	28
2.2.3. Thermoelectric Coolers (TEC).....	30
2.2.4. Fluid Loops.....	30
2.2.5. Active Thermal Architecture	31
2.3. Thermal Control Summary	32
3. Thermal analysis.....	33
3.1. Photovoltaic (PV) array thermal model	34
3.2. Airship envelope thermal model.....	35
3.3. Hydrogen thermal model	35
3.4. Simulation methodology	36

3.5. Governing equations.....	36
3.6. Solar Array.....	36
3.6.1. Ballonet Membrane.....	37
3.6.2. Lifting Gas.....	37
3.6.3. Ballonet Air.....	37
3.6.4. Solar Radiation.....	37
3.6.5. Infrared Radiation.....	37
3.6.6. Internal Radiation.....	38
3.6.7. Conduction.....	38
3.7. Boundary conditions.....	38
3.7.1. Mass and momentum conservation equations.....	38
3.7.2. Energy conservation equations.....	38
3.8. Solution method.....	41
4. Results and discussion.....	42
4.1. Average temperature of airship surface.....	43
4.2. Temperature distribution on airship surface.....	45
5. Conclusion.....	46
6. References.....	47

List of Figures

Figure 2-1: orbiting heating simplified overview. Credit: NASA.....	11
Figure 2-2: Electromagnetic spectrum showing the range of Thermal Radiation. Credit: NASA.	15
Figure 2-3: Flexible Thermal Straps. Credit: Thermal Management Technologies.....	18
Figure 2-4: Laird Tflex HD80000 series sheets (left) and Thermal Resistance vs. Pressure (right).....	20
Figure 2-5: A variety of thermal interface materials. Credit: Henkel Corporation.....	20
Figure 2-6: <i>Deployed Sunshield on CryoCube-1 (left)</i>	21
Figure 2-7: 100W deployable radiator (left) and uses graphite composite material for radiator shown on ESPA structure (right). Credit: Thermal Management Technologies.....	22
Figure 2-8: Q-Rad Deployable Radiator technology. Credit: Redwire.....	22
Figure 2-9: Rendering of an AMDROHP	23
Figure 2-10: Diagram of BIRD, heat pipe denoted. Credit: DLR	24
Figure 2-11: FlexCool conformable micro heat pipe before integrating with TechEdSat-10 DVB-S2 radio.Credit: Redwire Space.....	24
Figure 2-1: CubeSat Thermal Storage Unit. Credit: Thermal Management.....	25
Figure 2-1: Redwire Space's thermal energy storage technologies: (left) Q-Store and (right) Q-Cache. Credit: Redwire Space.	26
Figure 2-14: A comparison of cryocooler types. Credit: NASA.....	28
Figure 2-15: Configuration of primary mechanical ULP cryocooler compressor outlet to a heat component. Credit: Creare, Inc.....	29
Figure 2-16: (left) K508N 1/2 W Micro Cooler, and (right) K562S Mini cooler. Credit: Ricor-USA.....	29
Figure 2-17: (left) CryoTel DS1.5 1.4 W Cryocooler and (right) CryoTel MT F 5 W Cryocooler. Credit: Sunpower, Inc.	30
Figure 2-18: JT Compressor. Credit: Lockheed Martin	31
Figure 2-19: Conceptual operation of the ATA thermal control system. Credits: CSE/USU/ NASA/JPL.	32
Figure 2-20: From top left: ATA CubeSat prototype, ATA subsystem testing, ATA prototypes, UAM radiator with copper backing, UAM heat exchanger, Kevlar isolated Cryogenic Electro-optical prototype mount. Credit: CSE/USU/NASA/JPL.....	32
Figure 3-1: Thermal environment of stratospheric airship.	34
Figure 2-1: Heat transfer mechanism of PV array.	35
Figure 2-1: Heat transfer mechanism of airship envelope.....	35

Figure 3-4: Heat transfer mechanism of Hydrogen.....	36
Figure 3-5: Solar array model	36
Figure 3-6: Hexahedral mesh and coordinate system of the experiment airship.....	42
Figure 4-1: Hexahedral mesh and coordinate system of airship.....	43
Figure 4-2: Average temperature of airship surface.	44
Figure 4-3: Temperature distribution on airship surface; (a) 2 am; (b) 6 am; (c) 12 pm; (d) 18 pm	45

List of Tables

Table 2-1: HAPS Thermal Control Challenges	12
Table 2-2: Passive Thermal Technology.....	14
Table 2-3: Bolted Joint Thermal Conductance Design Guideline.....	19
Table 2-4: Active Thermal Systems.....	27
Table 4-1: Design index of the airship.....	42
Table 4-2: Material thermal properties of the airship.....	43

List of Acronyms

- (APG) Annealed Pyrolytic Graphite
- (ARC) Ames Research Center
- (ATA) Active Thermal Architecture
- (CFD) Computational Fluid Dynamics
- (FETS) Folding Elastic Thermal Surface
- (FOV) Field of View;
- (FOX) Flat-Plate Heat Pipe On-Orbit Experiment
- (HEC) High Efficiency Cooler
- (IFOV) Instantaneous Field Of View;
- (IR) Infrared
- (LPT) Linear Pulse Tube
- (MLI) Multi-Layer Insulation
- (MPFL) Mechanically Pumped Fluid Loop
- (MWIR) Midwave Infrared
- (OHP) Oscillating Heat Pipe
- (PFL) Pumped Fluid Loop
- (PGF) Pyrovo Pyrolytic Graphite Film
- (PGS) Pyrolytic Graphite Sheets
- (SI) International System of Units
- (SPOT) Standard Passive Orbital Thermal-Control
- (SST) Small Satellite Technology
- (SST) Small Satellite Technology
- (TAFTS) Two Arm Flexible Thermal Strap
- (TEC) Thermoelectric Coolers
- (TEC) Thermoelectric Coolers
- (TMT) Thermal Management Technologies
- (TMT) Thermal Management Technologies
- (TRL) Technology Readiness Level
- (TRL) Technology Readiness Level

(TSU) Thermal Storage Unit

(TSU) Thermal Storage Unit

(UAM) Ultrasonic additive manufacturing

(UAM) Ultrasonic additive manufacturing

(ULP) Ultra-Low Power

(ULP) Ultra-Low Power

(VDA) Vacuum Deposited Aluminium ...

(VDA) Vacuum Deposited Aluminium

Executive Summary

High altitude airships possess tremendous potential for long-endurance spot hovering platforms for both commercial and strategic applications. The energy system, which is mainly made up of solar array and regenerative fuel cell, is the key component of a high-altitude airship. The thermal effect is a major factor that affects the performance of the energy system of long endurance stratospheric vehicles. In this report, a conceptual design method focusing on the thermal and power characteristics of an energy system for stratospheric airships is proposed. The effect of thermal behaviour of solar array on the energy system is analysed. An optimized case is obtained on the consideration of power supply, thermal behaviours of hydrogen and solar array. Results show that the maximum temperature difference of the solar array may be reduced by about 20 K and the mass of payload can be improved by up to 5%.

The increase of airship applications makes it necessary for a comprehensive understanding of the thermal performance of stratospheric airships. A numerical model was proposed to simulate the thermal performance of a stratospheric airship with photovoltaic array, an analysis code was developed based on the thermal model and was verified by experimental data. A further inspection into the temperature field and flow field distribution of the airship was analysed in detail. The simulation results suggest that solar radiation can exert great influence on the thermal performance of the airship.

Airships and other lighter than air vehicles depend on a lifting gas to provide buoyancy. This lifting gas is subject to changes in temperature due to external heating which can affect its pressure and volume. Many airship designs contain ballonnet systems to allow the lifting gas to maintain a set pressure despite changes in temperature. This study improves the accuracy of airship thermal models by incorporating the effects of a ballonnet system. A transient thermal model based on a finite element discretisation for the structure and lumped averages for the gases was developed to account for the effects of a ballonnet system by formulating the first law of thermodynamics in conjunction with an ideal gas representation of the lifting gas and ballonnet air.

1. Introduction

HAPS (High Altitude Platform Stations) face two challenges related to Temperature management:

- The first challenge is the heating of H₂ gas in the sun and the thermal variations between a confined gas exposed to the sun and an external environment at another temperature, usually much lower. This affects the buoyancy and stability of the platform. Also need to discuss the concept and show some equations that account for solar radiation and Temperature effects on the gas dynamics.
- The second challenge is the Temperature of the onboard systems, such as the antenna, the batteries, the UCs and the electronics. These systems can overheat at low altitudes or freeze at high altitudes. This affects their performance and reliability. For this challenge, use a combination of different elements, such as air intakes, cold plates, heated wires, flow resistances, etc., that can either cool or heat the systems depending on the situation.

2. Thermal Control

All HAPS components have a range of allowable temperatures that must be maintained to meet survival and operational requirements during all mission phases. HAPS temperatures are determined by how much heat is absorbed, stored, or dissipated by the HAPS. Next figure shows a simplified overview of heat exchange from a satellite orbiting Earth, but the heating principles apply to any planet or body a HAPS orbits.

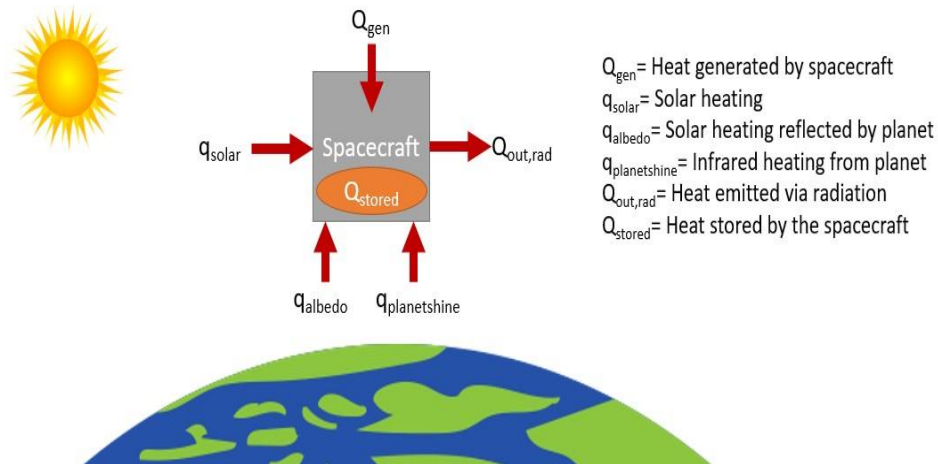


Figure 2-1: orbiting heating simplified overview. Credit: NASA.

The heat exchange depends on several factors listed below. Solar absorptivity and infrared (IR) emissivity are surface optical properties referenced below and are described further in section Paints, Coatings, and Tapes. Thermal control of a HAPS is achieved by balancing the energy as shown in Equation:

$$Q_{solar} + q_{albedo} + q_{planetshine} + Q_{gen} = Q_{stored} + Q_{out,rad}$$

Q_{gen} (heat generated by the HAPS) depends on the power dissipation of HAPS components.

The amount of q_{solar} (solar heating) absorbed by the HAPS depends on the solar flux, which is determined by distance to the sun, the surface area viewing the sun (view factor), and the solar absorptivity of that surface.

The amount of q_{albedo} (solar heating reflected by the planet) absorbed by the HAPS depends on the planet, the surface area viewing the planet (view factor), and the solar absorptivity of that surface.

The amount of $q_{planetshine}$ (IR heating from the planet) absorbed by the HAPS depends on the planet, the surface area viewing the planet (view factor), and the IR emissivity of that surface.

$Q_{out,rad}$ (heat emitted via radiation) includes the surface area designated as radiator space, the IR emissivity of the surface, and the difference in temperature between the HAPS radiator and the heat

sink to which it is dissipating, typically and most effectively deep space. $Q_{out,rad}$ also include heat lost through insulation or other surfaces not specifically intended to function as radiators.

Q_{stored} (heat stored by the HAPS), is based on the thermal capacitance of the HAPS.

Temperatures are regulated with passive and/or active thermal management technology and design methods. Many of the same thermal management methods used on larger HAPS are also applicable to HAPS and HAPS and given the increased interest in small HAPS over the last decade, some HAPS thermal control technologies have been miniaturized or otherwise adapted to apply to HAPS. Thermal control methods and technologies as applied to large HAPS are considered state-of-the-art for the purposes of this review but may have a Technology Readiness Level (TRL) value less than 9 for small HAPS applications.

Challenges of designing a thermal control system for a HAPS from several intrinsic properties, summarized in next table. Due to the small size and volume limitations inside the deployer or around deployable, there is often no room for multi-layer insulation (MLI) for CubeSats (as platform similar to HAPS). The thermal solution must be worked out as a coatings problem, exposing the CubeSat to more transient thermal behaviours.

Table 2-1: HAPS Thermal Control Challenges

HAPS Property	Challenge
Low thermal mass	The HAPS is more reactive to changing thermal environments.
Limited external surface area	There is less real estate to be allocated to solar cells, designated radiator area, and/or viewports required for science instruments.
Limited volume	There is less space for electronic components, science instruments, and thermal control hardware. Components can be more thermally coupled and it can be harder to isolate different thermal zones.
Limited power	There is less power available for powered thermal control technology.
Power Density	There is a big challenge to dissipate power as electronics are located close to each other, sometimes with no direct path to radiator.
MLI Edge Effects	MLI can "short" along the edges resulting in degraded performance, not specific to HAPS; more of a general HAPS issue.

The information described in this section is not exhaustive but provides an overview of current state-of-the-art thermal technologies and their development. TRL designations may vary with changes specific to the payload, mission requirements, reliability considerations, and/or the environment in which performance was demonstrated. Readers are highly encouraged to reach out to companies for further information regarding the performance and TRL of described technology.

2.1. State-of-the-Art – Passive Systems

Passive thermal control maintains component temperatures without using powered equipment. Passive systems are typically associated with low cost, volume, weight, and risk, and are advantageous to HAPS with limited, mass, volume, and power, like HAPS. MLI, coatings/surface finishes, interface conductance, heat pipes, sunshades, thermal straps, interface materials, and louvers are some examples of passive thermal control technology.

In addition to passive thermal control technology, structural and electrical design methods also contribute to managing the thermal environment, passively. These design methods include:

- Material selection or Structural component materials chosen based on needed heat transfer through the structure. A high or low thermal conductivity may be more advantageous based on the application.
- HAPS orientation
 - If orientation is not dictated by science objectives, changing the orientation of the HAPS can help maintain temperatures.
 - Changing orientation may only be needed during certain mission phases, such as science operation if larger amounts of heat are dissipated. This method is often used in conjunction with other thermal control methods, such as orienting the HAPS so that the radiator area can face deep space.
- Thermal interfaces:
 - Definition of the thermal contact between components through specific mounting methods can thermally isolate components or allow more heat to be transferred to a structural element (or radiator area) when each is needed. For example:
 - Heat transfer can be reduced by mounting a component through multiple stacked washers with low thermal conductivity.
 - Heat transfer can be increased by mounting components with more fasteners (if applicable) and can be further increased by using thermal interface materials between a component and mounting surface.
- Circuit board design considerations, include:
 - Copper layers within each board can be increased, in number or thickness, to conduct heat away from electrical components through the boards to their structural connection points.
 - Circuit boards can be mounted to increase heat transfer away from the boards to the structure, such as by mounting with wedge locks.

Next table is a list of current passive thermal control technology as applied to HAPS. One key factor to consider when choosing thermal control technology, both passive and active, is the temperature limits of the technology itself. The goal is to use the appropriate technology to maintain the temperatures of HAPS components within their limits, but the technology used to achieve this also has limits. It is recommended to verify that the technology used is applicable to the given design not only with respect to needed function, but to the environment (temperature limits) as well.

Table 2-2: Passive Thermal Technology

Manufacturer	Product	TRL
AZ Technology, MAP, Astral Technology Unlimited, Inc., Dunmore Aerospace, AkzoNobel Aerospace Coatings, Parker-Lord, Midterm	Paint and Coatings	7-9
Sheldahl, Dunmore, Aerospace Fabrication & Materials, 3M	Tapes	7-9
Sheldahl, Dunmore, Aerospace Fabrication & Materials	MLI Materials	7-9
NASA GSFC, Aerothreads, Aerospace Fabrication & Materials	MLI Blanket Fabrication	7-9
Space Dynamics Laboratory, Thermal Management Technologies, Boyd Corp., Technology Applications, Inc., Thermotive Technology, Redwire Space	Thermal Straps	7-9
Bergquist, Parker Chomerics, Aerospace Fabrication & Materials, AIM Products LLC, Intermark USA, Indium Corporation, Dow Corning, NeoGraf, Laird Technologies, Avantor (NuSil)	Thermal Interface Materials and Conductive Gaskets	7-9
Sierra Lobo, Aerospace Fabrication and Materials	Sun Shields	4 – 7
NASA Goddard Space Flight Center (GSFC)	Thermal Louvers	7-9
Aerospace Fabrication and Materials, Thermal Management Technologies, Redwire Space	Deployable Radiators	5-6
Aavid Thermacore, Inc., Advanced Cooling Technology, Inc., Redwire Space	Heat Pipes	7-9
Thermal Management Technologies, Active Space Technologies, Advanced Cooling Technology, Inc., Redwire Space	Phase Change Materials/ Thermal	7-9

	Storage Units	
Starsys, Redwire Space	Thermal switches	7-9
Thermal Management Technologies	Multifunctional Thermal Structures	4-5

2.1.1. Paints, Coatings, and Tapes

In a vacuum, heat is transferred only by radiation and conduction, with no convection. The internal environment of a fully enclosed small satellite is usually dominated by conductive heat transfer, while heat transfer to/from the outside environment is driven via thermal radiation. Many missions with electrical surface resistivity requirements drive the use of coatings with these properties to handle these surface charging concerns (this also applies to MLI). For HAPS missions where extensive use of MLI is not practical, a mixed use of several different coatings is needed to achieve optimal energy balance and thermal performance. There are also coatings that better approximate the use of MLI by being relatively low emissivity (such as 0.25) with a lower alpha (0.1) so they don't overheat in the sun. These are colloquially known as tailorable emittance coatings that involve some oxide depositions starting with a vacuum deposited aluminium (VDA) base to drive up the emissivity while keeping the alpha low.

The thermal radiation band of the electromagnetic spectrum is between 0.1 and 100 μm in wavelength, as shown in next figure. Outside of the thermal radiation waveband, electromagnetic energy generally passes through objects or has very little heat energy under practical conditions. Thermal analyses are typically conducted using a two waveband absorptance model which subdivides the thermal energy spectrum into solar ($< 3 \mu\text{m}$) and IR ($> 3 \mu\text{m}$) wavelengths.

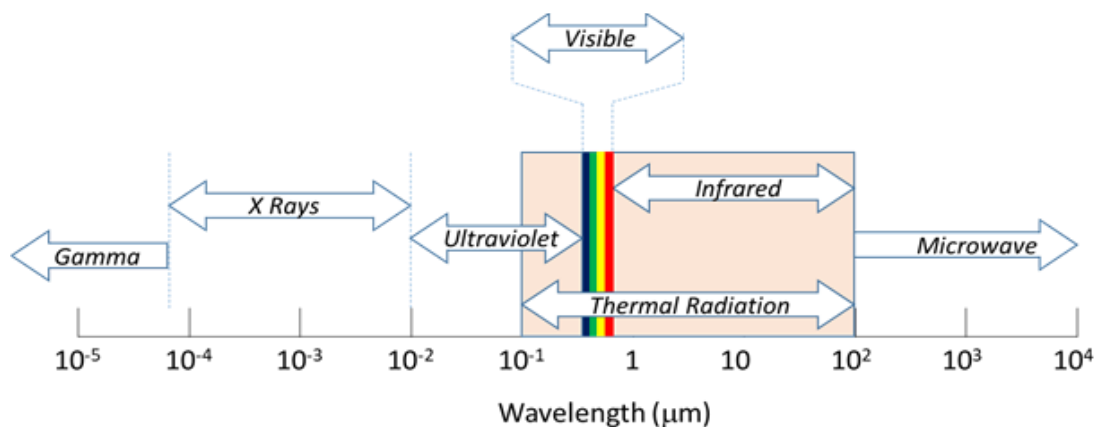


Figure 2-2: Electromagnetic spectrum showing the range of Thermal Radiation. Credit: NASA.

Thermal radiation heat transfer is controlled by using materials that have specific optical surface properties, namely: solar absorptivity and IR emissivity. Solar absorptivity governs how much incident heating from solar radiation a HAPS absorbs, while IR emissivity determines how much heat a HAPS emits to space, relative to a perfect blackbody emitter, and what fraction of thermal radiation from IR sources (e.g., the Earth, Moon, any particularly hot HAPS components) are absorbed by that HAPS surface.

The surface properties of a HAPS can be modified by adding specialized paints, coatings, surface finishes, or adhesive tapes, depending on the needs of the HAPS. For example, matte black paint has a high solar absorptivity and high IR emissivity for surfaces required to absorb a high percentage of solar heating and emit a high percentage of HAPS heat. Alternatively, matte white paint has a low solar absorptivity and high IR emissivity (1) for surfaces required to absorb a low percentage of solar heating and emit a high percentage of HAPS heat (e.g., radiator). Second-surface silver Fluorinated Ethylene Propylene (FEP) tapes offer excellent performance as radiator coatings, reflecting incident solar energy (low solar absorptivity) while simultaneously emitting HAPS thermal energy efficiently (high IR emissivity). The selection between paints, coatings, and tapes depends on the application. Tape is typically easy to apply and remove, is comparatively inexpensive, and has a longer usable lifetime than paint. Tape can also be added later in the assembly process if changes to thermal control need to be made after the HAPS has already begun assembly. Some tapes, however, must be handled carefully to maintain optical properties and can be difficult to bond properly to curved surfaces. Coatings and paints must often be applied earlier in the assembly process but can cover non-flat surfaces more easily. However, some paints, like Parker-Lord's Aeroglaze 306/307, are expensive and require extensive and highly specialized processes to apply. Different options may also have different temperature limits. All these factors must be considered with regard to the needed application when selecting the final solution.

AZ Technology, MAP, Astral Technology Unlimited, Inc., Parker-Lord, Inc., Sheldahl, and AkzoNobel Aerospace Coatings manufacture thermal paint, coatings, and tapes for aerospace use that have been demonstrated on multiple small HAPS missions. Most manufacturers have catalogues and/or guidebooks that provide detailed product information, including optical properties, and application guidance (for example, Sheldahl provides "The Red Book,") to aid design selection.

One example, BioSentinel, a 6U SmallSat in development at NASA Ames Research Center (ARC) that is currently slated to be launched as a secondary payload on the Artemis I mission (2022), makes extensive use of Sheldahl metallized tape coatings and second-surface silvered FEP tapes to control its external thermal radiative properties and overall energy balance (4). Another example, Picard, a 150 kg HAPS, used white paint on the Sun pointing face to reduce the amount of solar flux absorbed and lower temperatures. For most small HAPS projects to date, adhesive tapes, such as silver FEP, or other standard surface finishes (e.g., polishing, anodize, Alodine) have been the preferred choices.

2.1.2. Multi-layer Insulation

A MLI blanket is typically comprised of multiple inner layers of a thin material with low IR emissivity (usually 10 to 20 layers) and a durable outer layer. The amount of radiative heat transfer allowed is

limited by the many layers of reflectors. The low IR emissivity layers are either embossed or alternated with thin netting to limit conduction through the layers. Perforations may be added to allow the MLI to vent trapped gas once arriving on-orbit, although this can also be achieved via edge venting. MLI is used as a thermal radiation barrier to both protect HAPS from incoming solar and IR flux, and to prevent undesired radiative heat dissipation to space. It is commonly used to maintain temperature ranges for components in-orbit.

MLI is delicate and performance drops drastically if compressed (causing a thermally conductive “short circuit”), so it should be used with caution or avoided altogether on the exterior of small satellites that fit into a deployer (e.g., P-POD, NLAS). MLI blankets can also pose a potential snagging hazard in these tight-fitting, pusher-spring style deployers. Additionally, MLI blankets tend to drop efficiency as size decreases because heat transfer through the blanket increases closer to the blanket edges, and the specific attachment method has a large impact on performance because attachment to the HAPS creates a heat path.

Due to these challenges, MLI generally does not perform as well on small HAPS (more specifically CubeSat form factors) as on larger HAPS. Surface coatings are typically less delicate and more appropriate for the exterior of a small HAPS that will be deployed from a dispenser. Internal MLI blankets that do not receive direct solar thermal radiation can often be replaced by a variety of low emissivity tapes or coatings that perform equally well in that context, using less volume and at a potentially lower cost.

Dunmore Aerospace provides an option for CubeSat developers to make their own MLI blanket with Satkit (3). Satkit provides Dunmore’s STARcrest MLI materials cut into manageable sizes, including a roll of outer layer material, a larger roll of inner layer material, and polyimide tapes for assembly and edge binding. The materials included in the kit have been flown in spaceflight applications before, but Satkit is currently TRL 6. Dunmore also offers polyimide film tape and MLI tape designed to insulate wires and cables on HAPS and is TRL 7.

2.1.3. Thermal Straps

A thermal strap is a flexible, thermally conductive link added between a heat source and sink to conductively transfer heat. They are often used between high heat dissipating chips or components and a chassis wall or other radiator surface. Their flexibility prevents the addition of structural loads. Thermal straps can be made metal, traditionally copper or aluminium, or high conductivity carbon materials, such as graphite. They can be formed of multiple foil sheets or wound cables (also referred to as ropes and braids), with end blocks at each end to hold the sheets/cables in place and to mount or otherwise attach to the needed surfaces. Straps with more than two end blocks and multiple material combinations can also be produced and have been used on large HAPS.

There are multiple companies that manufacture thermal straps for spaceflight. For example, Thermal Management Technologies manufactures standard flexible thermal straps in aluminium and copper foil layers or copper braids as shown in figure. Custom thermal straps are also commonly fabricated and tested. Space Dynamics Laboratory (SDL) has pioneered solderless flexible thermal straps that contain no solder, epoxy, or other filler materials to maximize thermal performance. Figure shows a

comparison of the as-tested conductance for the same strap geometry fabricated with three different foil materials of aluminium, copper, and pyrolytic graphite sheets (PGS). SDL supplied Utah State University with a PGS strap for the Active Thermal Architecture (ATA) project sponsored by the Small HAPS Technology (SST) program. A follow-on to this ATA project is referenced in the cryocooler section.

Advances in thermal straps are being developed to further increase heat transfer capability. Aavid Thermacore, Boyd Corporation's thermal division, has designed thermal straps using their patented k-core technology that has an annealed pyrolytic graphite (APG) core within an encapsulating structure. These have greater conduction efficiency compared to traditional aluminium straps as the k-Core increases the overall thermal conductivity (5). This technology has been fully designed and tested and is TRL 5 for small HAPS application.



Figure 2-3: Flexible Thermal Straps. Credit: Thermal Management Technologies.

Thermotive Technology developed the Two Arm Flexible Thermal Strap (TAFTS) that is currently flying on JPL's Portable Remote Imaging Spectrometer (PRISM) instrument. Space infrared cameras require extremely flexible direct cooling of mechanically sensitive focal planes. The design of TAFTS uses three swaged terminals and a twisted section that allows for significant enhanced elastic movement and elastic displacements in three planes, while a more conventional strap of the same conductance offers less flexibility and asymmetrical elasticity (7). While infrared cameras have flown on small HAPS missions, the TAFTS design has not been employed on a HAPS.

Redwire Space offers flexible thermal strap solutions that use high-k graphite material, such as their Q-Strap. By layering sheets of graphite material into a traditional layered heat strap, the heat transfer is increased while the mass of the strap system is decreased. For the same conductance, fewer layers can be used compared to traditional aluminum or copper thermal straps, minimizing mass and volume. The Q-Strap can be manufactured in various lengths and widths, has an inplane thermal conductivity of ~ 700 W/m-K and is anywhere from 1.4 to 3.5 kg/m².

2.1.4. Thermal Contact Conductance and Bolted Joint Conductance

Bolted joints experience non-uniform pressure creating a more complex heat transfer scenario. The conductance will depend on screw size, torque, surface properties and other values. The conductance can be varied by changing torque, surface properties and finishes and materials. Table 7-3 provides conductances for various screws (9).

Table 2-3: Bolted Joint Thermal Conductance Design Guideline

Screw Size	Conductances [W/K]	
	Small Stiff Surface	Large Thin Surfaces
2-56	0.21	0.105
4-40	0.26	0.132
6-32	0.42	0.176
8-32	0.80	0.264
10-32	1.32	0.527
1/4-28	3.51	1.054

2.1.5. Thermal Interface Materials and Conductive Gaskets

Thermal interface materials are inserted between two components to increase the conductive heat transfer between them. They are often made as a sheet or pad of material to be sandwiched between surfaces, but there are many different types that vary in material, thickness, thermal conductivity, temperature limits, and vacuum-compatibility. Thermal interface materials can also be a grease or paste.

Thinner sheets of materials are commonly used between heat dissipating electronics boxes and mounting surfaces to thermally sink the hot components to a colder surface and reduce the temperature of the electronics. The performance of these types of materials depends on reaching a certain contact pressure between components to ensure the needed heat transfer. Laird Performance Materials has developed many different types of thermal interface materials for a variety of applications. For example, their Tflex series, shown in next figure, is about 1 to 5 mm thick with a thermal conductivity of 6 W mK^{-1} (10), whereas their Tgon series of materials are about 0.13 to 0.5 mm thick with a thermal conductivity of 5 W mK^{-1} (2).

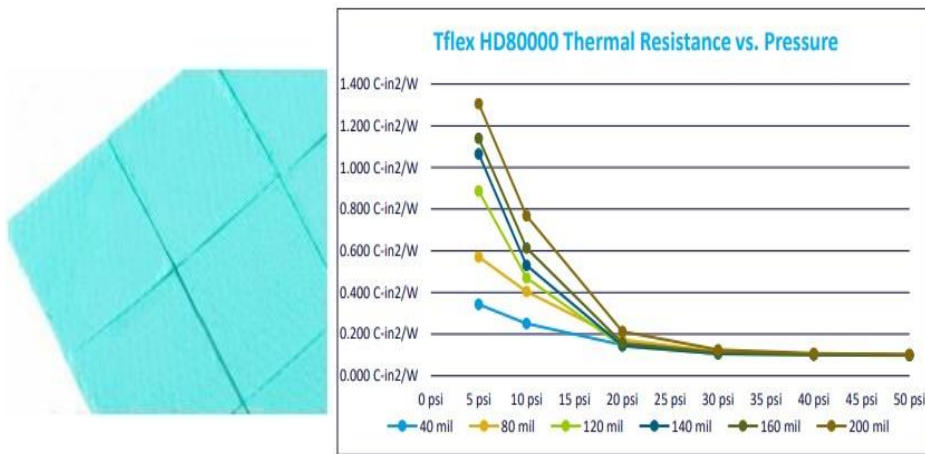


Figure 2-4: Laird Tflex HD80000 series sheets (left) and Thermal Resistance vs. Pressure (right). Credit: Laird Performance Materials.

Thicker pad-like materials, such as Henkel brand GAP PADs®, are often used between high heat dissipating chips on an electronics boards and the electronics enclosure. These are also made to fit a variety of applications, with varying material, thickness, conformability, tear-resistance, electrical isolation, thermal conductivity, and more (2). Several additional thermal interface materials developed by Henkel Corporation are shown in figure 7.9.

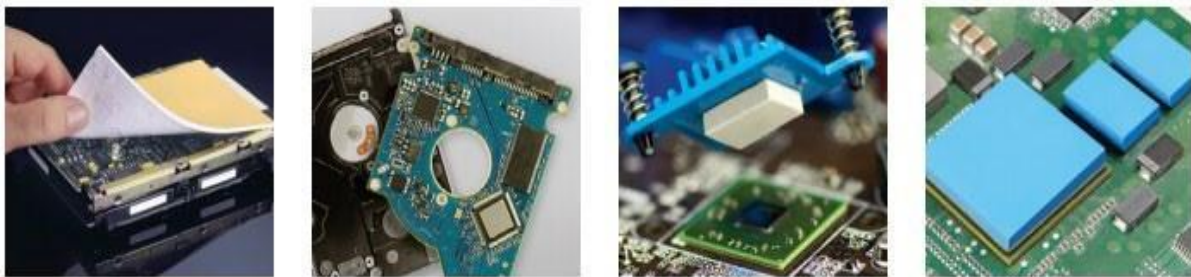


Figure 2-5: A variety of thermal interface materials. Credit: Henkel Corporation.

2.1.6. Sunshields

A sunshield, or sunshade, is an often deployed device made up of a material with low solar absorptivity that reduces the amount of incident solar flux impinging a HAPS, by blocking the view to the sun. Sunshields are commonly used for HAPS thermal control, although only recently on small HAPS. Sierra Lobo developed a deployable sunshield that flew on CryoCube-1, shown in figure 7.10, which was launched on Dragon CRS19 in February 2020. In low-Earth orbit, this sunshield can support a multiple month-long duration lifetime and can provide temperatures below 100 K and below 30 K with additional cooling (2).

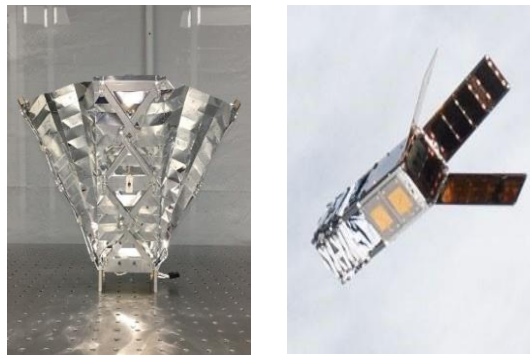


Figure 2-6: *Deployed Sunshield on CryoCube-1 (left) and CryoCube-1 in orbit with shield stowed (right).*
Credits: Sierra Lobo (left) and NASA (right).

2.1.7. Thermal Louvers

Thermal louvers are thermally activated shutters that regulate how much heat the louvered surface can dissipate. As the louvers open, the average IR emissivity of the surface changes, changing how much heat the surface dissipates. Full-sized louvers on larger HAPS have high efficacy for thermal control, however, integration on small HAPS is challenging. Typical HAPS louvers are associated with a larger mass and input power, which are both limited on small HAPS.

Although commonly defined as active thermal control, here we consider louvers as a passive thermal control component because the CubeSat-adapted design considered does not require a power input from the HAPS. NASA GSFC developed a passive thermal louver that used bimetallic springs to control the position of a single flap so when the temperature of the HAPS rises, the springs expand and open the louver to modify the average IR emissivity of the exterior surface. This louver was developed as a technology demonstration on a 6U CubeSat, Dellinger, which was released from the International Space Station (ISS) into low-Earth orbit in late 2017 (2), however performed no actual thermal control function on the CubeSat.

2.1.8. Deployable Radiators

A radiator is a dedicated surface for dissipating excess heat via radiative heat transfer and has a high IR emissivity and low solar absorptivity, an optical property combination typically referred to as “radiator properties.” A deployable radiator is stowed during transit or when the radiator is not needed and deployed when excess heat dissipation is required. Deployable radiators on small HAPS can be challenging due to volumetric constraints. While paint has been widely used to create efficient radiator surfaces on larger HAPS, the relatively limited available external surface area on HAPS that already have body-mounted solar cells reduces the potential for creating dedicated radiative surfaces. For a system that requires a large amount of heat dissipation, a passive deployable radiator would greatly enhance thermal performance by increasing the available radiative surface area. Since deployable radiators may be needed because of a lack of radiator surfaces on the HAPS body due to body-mounted solar cells, an alternate approach (perhaps more common for CubeSats) is to use the chassis body as the radiator area and have a deployable solar array. Also, deployed solar arrays would

be able to radiate off a high emissivity/low solar absorptance backside for improved thermal management of the array. There has been steady development in this technology over the last five years and radiator designs for HAPS have improved to TRL 5.

Thermal Management Technologies has developed thermally efficient deployable radiators for small HAPS that integrate a radiator surface with a high-conductance hinge. The thermally conductive hinge causes minimal temperature gradients between the radiator and HAPS; thus, the radiator can operate near HAPS temperatures. Next figure: shows the radiator design. The radiating surface mass reduction and increased stiffness, where the typical radiator uniformity is less than $0.1^{\circ}\text{C W}^{-1}\text{m}^{-1}$. This technology is currently in the development and testing phase (2)

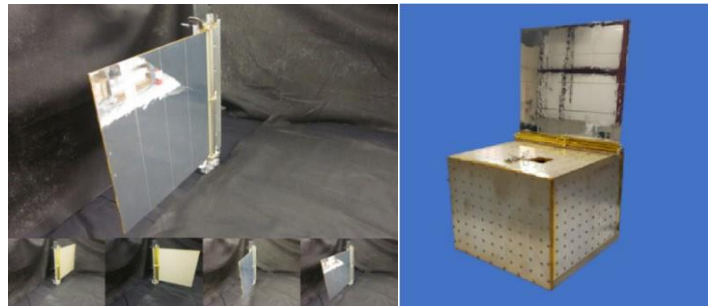


Figure 2-7: 100W deployable radiator (left) and uses graphite composite material for radiator shown on ESPA structure (right). Credit: Thermal Management Technologies

Thermotive is researching the Folding Elastic Thermal Surface (FETS), a deployable passive radiator for hosted payload instruments and CubeSats. Originally conceived as a thermal shield and cover for a passive cooler (cryogenic radiator) on JPL's MATMOS mission, this proposed concept is being modified as a deployable radiator for small HAPS.

The Q-Rad deployable radiator offered by Redwire Space leverages a lightweight high-strain composite-based deployment approach and incorporates flexible, high-k graphite material to transport heat effectively across the hinge line, making it a lightweight and modular solution. For a 20 cm length radiator prototype, an estimated 300 W/m could be rejected with a rejection temperature of 100 °C based on the 80% fin efficiency. Next figure shows one example of a deployable thermal dissipation technology.

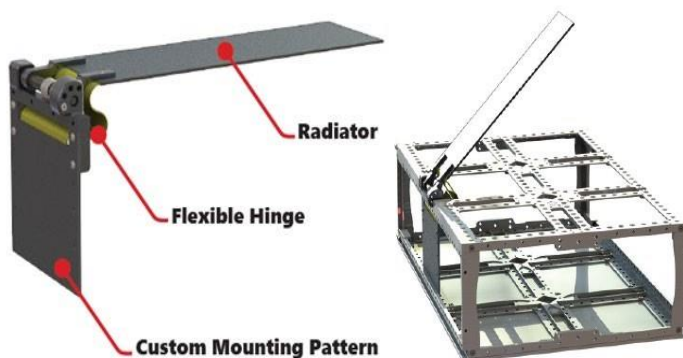


Figure 2-8: Q-Rad Deployable Radiator technology. Credit: Redwire Space.

A novel deployable radiator is being developed by JPL, California Polytechnic San Luis Obispo, and California State Los Angeles. At the core of this technology is an Additively Manufactured Deployable Radiator with embedded Oscillating Heat Pipes (AMDROHP) that enables heat to be efficiently transported across moving interfaces. The current AMDROHP radiator design is shown in next figure and consists of an evaporator and a condenser plate, and a series of flexible joints connecting the two plates. AMDROHP can be stowed within a 3U CubeSat and can be passively deployed without use of an actuator. AMDROHP technology is currently in the testing phase and further design optimization is ongoing. AMDROHP is funded by NASA's SST program in the 2020 cohort of the HAPS Technology Partnerships initiative.

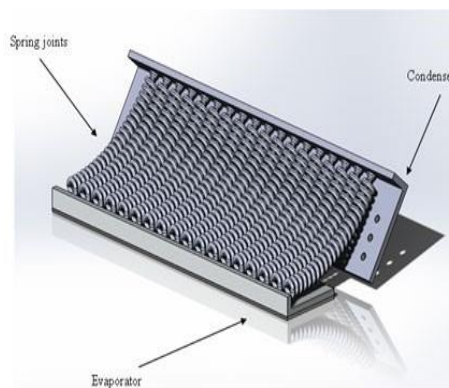


Figure 2-9: Rendering of an AMDROHP radiator design. Credits: California State

2.1.9. Heat Pipes

A traditional heat pipe is a passive device comprised of a metal container (pipe) that holds a liquid under pressure and has a porous wick-like structure within the container. When heat is applied to one end of the tube, the liquid inside the tube near the hot end vaporizes into a gas that moves through the tube to the cooler end, where it condenses back into a liquid. The wick transports the condensed liquid back to the hot end via capillary action. There are also more complicated and non-passive types of heat pipes such as variable conductance, diode, and loop heat pipes, which are not further explained in this document.

Heat pipes are an efficient passive thermal transfer technology, where a closed-loop system transports excess heat via temperature gradients, typically from electrical devices to a colder surface, which is often either a radiator itself, or a heat sink that is thermally coupled to a radiator. Traditional constant conductance heat pipes are cylindrical in shape with a grooved inner wick, like those used on Bi-Spectral Infrared Detection (BIRD), a 92 kg satellite launched in 2001, to join satellite segments (2), see next figure.

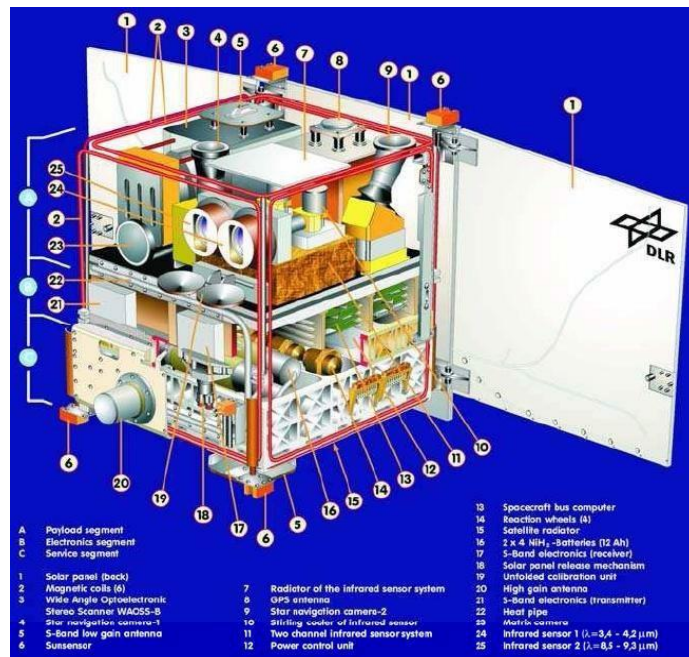


Figure 2-10: Diagram of BIRD, heat pipe denoted.

Credit: DLR

Heat pipes can also be configured as flat plates with tubing sandwiched between two plates and charged with a working fluid inside. SDS-4, a 50 kg small HAPS launched in 2012, incorporated the Flat-Plate Heat Pipe On-Orbit Experiment (FOX), developed at JAXA (2).

Redwire Space has multiple forms of heat pipe thermal transport solutions to provide relatively high heat load transport with high heat acquisition across a satellite’s architecture including flat heat pipes and oscillating heat pipes. The FlexCool is a bent, flat heat pipe developed as a cross between a heat pipe and a thermal strap that can be customized for higher heat fluxes by increasing the thickness.

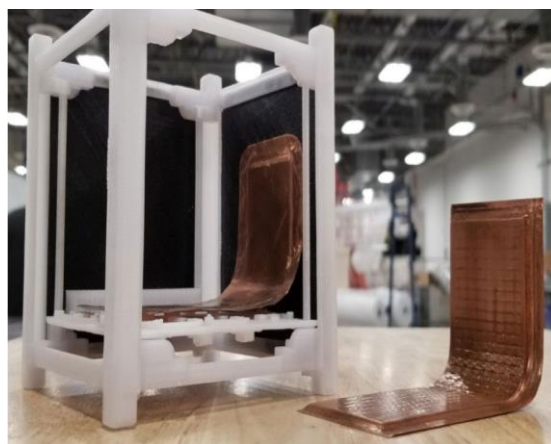


Figure 2-11: FlexCool conformable micro heat pipe before integrating with TechEdSat-10 DVB-S2 radio. Credit: Redwire Space.

It has ten times the thermal conductivity of copper, while being 90% lighter, and up to 6 W/cm^2 at 1 mm thick. The FlexCool heat pipe flew on TechEdSat-10, a 6U CubeSat deployed from the ISS in 2020, to thermally manage the radio. An image of this technology in a 1U CubeSat model is shown in figure above. Another solution offered by Redwire Space is the Flex-OHP, an oscillating heat pipe (OHP) with thermal transport technology that can accommodate higher heat fluxes as it has a higher effective thermal conductance compared to solid-state solutions, at a total conductance of 1.7 W/K at $50 \text{ }^\circ\text{C}$.

2.1.10. Phase Change Materials/ Thermal Storage Units

A phase change material used as a thermal storage unit is made up of a material (e.g., wax) within a metal housing. A heat source is attached to the housing so that, as the source conducts heat to the enclosure, the phase change material within absorbs the energy as it changes phase (usually from solid to liquid). Then, as the heat source energy output reduces, the phase change material releases the energy as it changes back to its initial phase (usually from liquid to solid). Owing to the low thermal conductivity of the phase change material, the metal housing must conduct heat into the phase change medium for efficient solidification or melting. Thermal storage units are typically used with components that will experience repeated temperature cycling or to slow down the temperature transient caused by a high heat dissipation event, or a temporary change in the environment such as an eclipse. They can be challenging to apply to HAPS because of the extra mass of the housing needed.

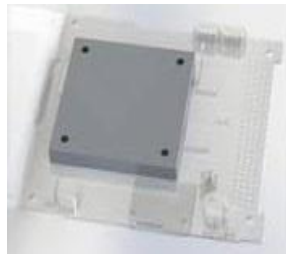


Figure 2-12: CubeSat Thermal Storage Unit.
Credit: Thermal Management

Thermal Management Technologies has developed a phase-changing thermal storage unit (TSU) that considers desired phase-change temperatures, interfaces, temperature stability, stored energy, and heat removal methodologies, as shown in figure above. This device will allow the user to control temperature peaks, stable temperatures and/or energy storage (2).

Redwire Space has developed multiple phase change materials (PCM)-based thermal energy storage panels that are of the CubeSat form factor, allowing them to be easily stacked in between critical components (20). Q-Store shown in figure 7.17 (left) and Q-Cache shown in figure 7.17 (right) are two examples of thermal energy storage technology solutions. Both Q-Store and Q-Cache are tailorable thermal storage solutions that dampen thermal swings. Either one can be customized to fit complex shapes, and both have thermal vias embedded into their design to assist with the thermal path challenges inherent to paraffin-wax-based technologies (which have very low thermal

conductivities). Q-Store is a brazed technology solution, whereas Q-Cache is an additively manufactured option.

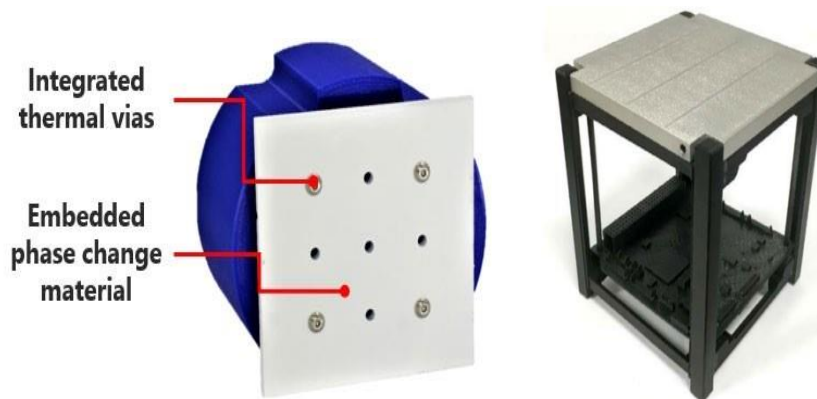


Figure 2-13: Redwire Space's thermal energy storage technologies: (left) Q-Store and (right) Q-Cache. Credit: Redwire Space.

2.1.11. Thermal Switches

A thermal switch is a device that switches a heat conduction path between either a strong thermal coupling or weak thermal coupling (thermal isolation) as needed to control the temperature of heat producing components. A switch typically connects a heat producing component and a low temperature sink, such as a radiator. Heat switches differ from thermostats in that they passively modulate a thermal coupling while thermostats modulate heater circuits (2). Part of the challenge in integrating a thermal switch in HAPS is that they take up additional space between a component and heat sink. Typical, heat switches may provide a conduction ratio of 10:1 with a technology goal of 100:1 (2).

2.1.12. Multifunctional Thermal Structures

A newer development in passive thermal control for small HAPS are multi-functional thermal structures. These integrate thermal control capabilities directly into the structure. This is particularly advantageous for small HAPS due to strict mass and volume constraints. Currently, Thermal Management Technologies has adapted its multifunction heat spreading structure technology, scaled it to smaller satellite configurations, and called it Standard Passive Orbital Thermal-control (SPOT) Structures. SPOT Structures come in four standard configurations: 6U, 12U, Launch U, and ESPA (2). Each incorporates heat-spreading technology that improves the ability to radiate waste heat. They incorporate features such as low mass, high stiffness/strength, and integrated heat pipes. This new technology is at TRL 4.

2.2. State-of-the-Art – Active Systems

Active thermal control methods rely on input power for operation and have been shown to be more effective in maintaining tighter temperature control for components with stricter temperature requirements or higher heat loads (2). Typical active thermal devices used on large-scale HAPS

include electrical resistance heaters, cryocoolers, thermoelectric coolers, and fluid loops. Electrical heaters are usually easily integrated into HAPS architectures as they do not typically use much mass or volume. Heaters are frequently used in all space applications, including small and large satellites, so they are often included as passive thermal control technology. Other active systems are challenging to integrate into CubeSats and HAPS because of the power, mass, and volume needs associated with each given technology.

Until HAPS designers can miniaturize existing actively controlled thermal techniques and reduce power requirements or increase available HAPS power, the use of active thermal systems in small HAPS will be limited.

Current state-of-the-art active thermal technologies for HAPS are shown in next Table.

Table 2-4: Active Thermal Systems

Manufacturer	Products	TRL
Minco Products, Inc., Birk Manufacturing, All Flex Flexible Circuits, LLC., Fralock, Tayco Engineering, Inc., Omega	Electrical Heaters	7-9
Ricor-USA, Inc., Create, Sunpower Inc., Northrop Grumman, NASA Jet Propulsion Lab, and Lockheed Martin Space Systems Company	Cryocoolers	5-6
Marlow, TE Technology Inc., Laird	Thermoelectric Coolers (TEC)	7-9
Lockheed Martin	Fluid Loops	4-5
NASA Small HAPS Technology program	Active Thermal Architecture (ATA)	4-6

2.2.1. Heaters

Electrical resistance heaters used on small HAPS are most often Kapton heaters, which consist of a polyimide film with etched foil circuits that produce heat when a current is applied. Kapton heaters also often have a pressure sensitive adhesive on one side for easy application. Heaters are typically controlled by a thermostat or temperature sensor and used in cold environments to maintain battery temperature, typically the component with the narrowest temperature limits. The low mass of HAPS requires little additional heater power to maintain temperature limits, and so heaters do not typically need to be very high power to effectively manage temperatures.

The 1U CubeSats Compass-1, MASAT-1, and OUTFI-1 each required an electrical heater attached to the battery in addition to passive control for the entire HAPS system to maintain thermal regulation in eclipses (2). Additionally, as biological payloads become more common on small HAPS, their temperature limits must be considered and maintained as well. NASA ARC biological nanosats

(GeneSat, PharmaSat, O/OREOS, SporeSat, EcAMSat, and BioSentinel) all used actively controlled heaters for precise temperature maintenance for their biological payloads, with closed-loop temperature feedback to maintain temperatures.

2.2.2. Cryocoolers

Cryocoolers are refrigeration devices designed to cool around 100K and below. A summary of cryocooler systems is given in next figure and a detailed review of the basic types of cryocoolers and their applications is given by Radebaugh (2). The first two systems (a) and (b) are recuperative cycles, and (c), (d), and (e) are regenerative cycles. Cryocoolers are used on instruments or subsystems requiring cryogenic cooling, such as high precision IR sensors. Instruments such as imaging spectrometers, interferometers and midwave infrared (MWIR) sensors require cryocoolers to function at extremely low temperatures. The low temperature improves the dynamic range and extends the wavelength coverage. The use of cryocoolers is also associated with longer instrument lifetimes, low vibration, high thermodynamic efficiency, low mass, and supply cooling temperatures less than 50K (2). Cryocoolers on small HAPS are still a new concept, however, there have been two CubeSats with cryocooling on board. Lunar IceCube, a 6U secondary payload on-board Artemis I and developed by Morehead State University, will use a 600 mW cryocooler for its BIRCHES point spectrometer (28). Below are cryocooler descriptions on from commercial vendors.

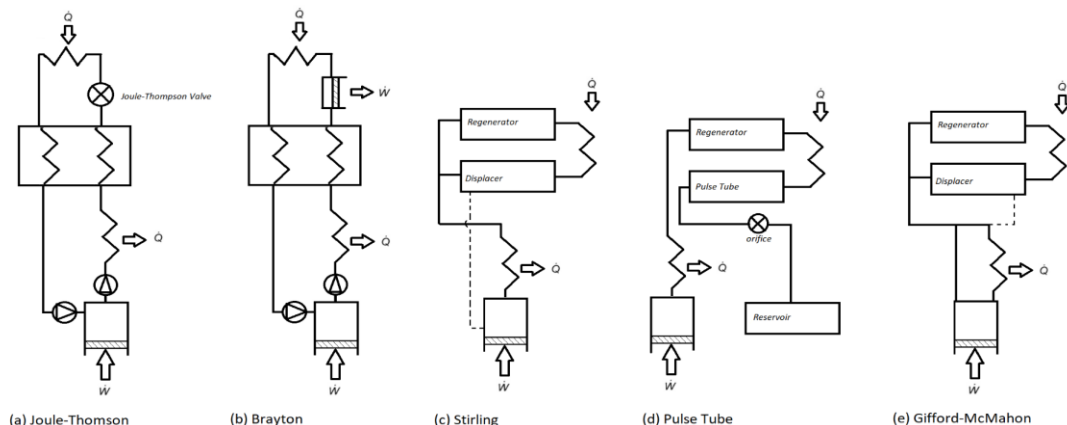


Figure 2-14: A comparison of cryocooler types. Credit: NASA.

Creare developed an Ultra Low Power (ULP) single stage, turbo-Brayton cryocooler that operates between a cryogenic heat rejection temperature and the primary load temperature (figure above). The cryocooler includes a cryogenic compressor, a recuperative heat exchanger, and a turboalternator. The continuous flow nature of the cycle allows the cycle gas to be transported from the ejection radiator at the warm end of the cryocooler and from the turboalternator outlet to the object to be cooled at the cold end of the cryocooler (2). This cryocooler is designed to operate at cold end temperatures of 30 to 70K, with loads of up to 3 W, and heat rejection temperatures of up to 210K by changing only the charge pressure and turbo machine operating speeds. This technology has completed testing and fabrication and is TRL 6. The development of this technology has not specifically targeted small satellite applications, but with its comparatively low power requirements could be adapted to HAPS in the future. An additional benefit is it produces negligible vibration with minimal impact on pointing accuracy or imaging.

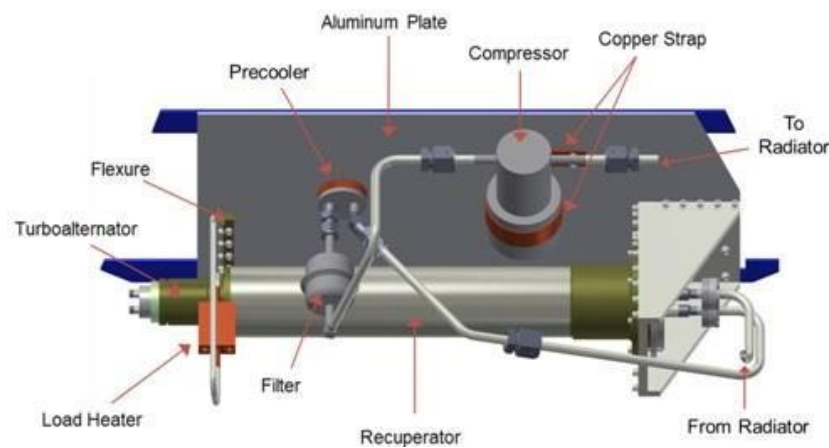


Figure 2-15: Configuration of primary mechanical ULP cryocooler compressor outlet to a heat component.

Credit: Creare, Inc.

A reverse turbo-Brayton cryocooler that produces negligible vibration is also being developed by Creare. This technology uses a continuous flow of gas to transport heat from the active elements of the cryocooler to the objects to be cooled and to heat rejection surfaces.

Ricor-USA, Inc. developed the K562S, a rotary Sterling mini micro-cooler. It has a cooling capacity of 200 mW at 95 K and 300 mW at 110K. It has been used in several small gimbals designed for military applications (2). Ricor also developed K508N, a Sterling 1/2 W micro cooler that has a cooling capacity of 500 mW at 77 K and 700 mW at 77K that is suitable for small HAPS (31). These coolers, shown in next figure, are TRL 6 for small HAPS applications.



Figure 2-16: (left) K508N 1/2 W Micro Cooler, and (right) K562S Mini cooler. Credit: Ricor-USA.

Sunpower, Inc. developed the CryoTel DS1.5 Sterling Cryocooler (next figure) features a dual-opposed-piston pressure wave generator and a separate cold head to minimize exported vibration and acoustic noise, with a nominal heat lift of 1.4 W at 77K using 30 W power with a 1.2 kg mass (2). Sunpower also offers MT-F, a mini-cooler that has a nominal heat lift of 5 W at 77K, using 80 W power with a total mass of 2.1 kg. So far, these units have not been used in small HAPS applications but are candidates given their size and performance.



Figure 2-17: (left) CryoTel DS1.5 1.4 W Cryocooler and (right) CryoTel MT F 5 W Cryocooler. Credit: Sunpower, Inc.

Northrop Grumman designed a Micro Pulse Tube cooler that is a split-configuration cooler that incorporates a coaxial coldhead connected via a transfer line to a vibrationally balanced linear compressor. This micro compressor has been scaled from a flight proven, high efficiency cooler (HEC) compressor, although it has not operated on a HAPS. It has a TRL of 6. The cooler has an operational range of 35 to 40K and a heat rejection temperature of 300K, using 80 W of input power, has 750 mW refrigeration at 40K, and a total mass of 7.4 kg (2).

Lockheed Martin Space Systems Company has engineered a pulse tube micro-cryocooler, a simplified Sterling cryocooler consisting of a compressor driving a coaxial pulse tube coldhead. The unit has a mass of 0.345 kg for the entire thermal mechanical unit and is compact enough to be packaged in a ½U CubeSat (2). After qualification testing, the microcooler is at TRL 6 and is compatible with small HAPS missions.

Thales Cryogenics has also developed a Linear Pulse Tube (LPT) cryocooler that has gone through extensive testing by JPL. The Thales LPT9510 cryocooler has an operating temperature range of -40 to 71°C, an input power of <85 W, and a total unit mass of 2.1 kg. The unit has no flight heritage but has undergone extensive testing and is TRL 6 (2)

2.2.3. Thermoelectric Coolers (TEC)

TECs are miniature solid-state heat pumps which provide localized cooling via the Peltier effect, which is cooling resulting from passing electric current through a junction formed by two dissimilar metals. TECs have been used to cool star trackers, IR sensors and low noise amplifiers. Advantages of TECs are that they have no moving parts, are reliable, noiseless, lightweight, and compact. Their use is limited by low efficiency below temperatures of 130K and low performance with large temperature differences. Furthermore, the TECs are fragile to mount and highly sensitive to thermal expansion stresses. External stresses can be mitigated by adding a conductive strap on the cold side (2).

2.2.4. Fluid Loops

A pumped fluid loop (PFL) consists of a circulating pump that moves a liquid through tubing connected to a heat exchanger and heat sink. A heat source is mounted to the heat exchanger and the pumped fluid carries the heat from the source to a heat sink, typically a radiator, and then the cooled fluid is returned to the heat source to continue providing cooling. A PFL is capable of cooling

multiple locations via forced fluid convective cooling. Mechanically pumped fluid loops (MPFL) are not typically used on HAPS because they are associated with high power consumption and mass.

Lockheed Martin Corporation is developing a low mass circulator pump for a closed-cycle Joule Thomson cryocooler, as shown in next figure. With an overall mass of 0.2 kg, it can circulate gas as part of a single-phase or two-phase thermal management system using 1.2 W of electrical power and can manage around 40 W of HAPS power as a single-phase loop, or several hundred Watts of HAPS power as part of a 2-phase loop. The compressor went through applicable testing with a compression efficiency of 20 – 30% in a 2016 study (2). This design is TRL 4.

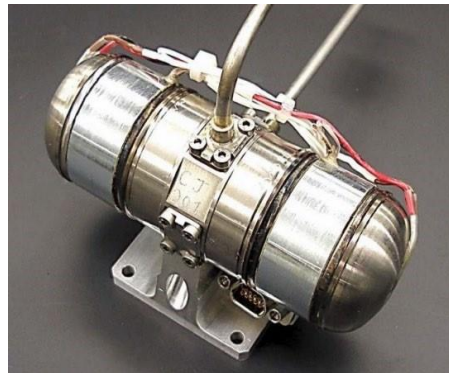


Figure 2-18: JT Compressor. Credit: Lockheed Martin

2.2.5. Active Thermal Architecture

The Active Thermal Architecture (ATA) system is an advanced, active thermal control technology for small satellites in support of advanced missions in deep space, helio-physics, earth science, and communications. The ATA technology is capable of high-power thermal rejection, and zonal temperature control of satellite busses, payloads, and high-energy density components. The ATA project was developed by the Center for Space Engineering at Utah State University (CSE, USU) and funded by the NASA SST program in partnership with JPL.

The ATA is a sub 1U two-stage active thermal control system targeted at 6U CubeSat form factors and larger. The first stage consists of a mechanically pumped fluid loop (MPFL). A micro-pump circulates a single-phase heat transfer fluid between an internal heat exchanger and a deployed tracking radiator. The second stage is composed of a miniature tactical cryocooler, which directly provides cryogenic cooling to payload instrumentation. The conceptual operation of the ATA system is shown in next figure.

Ultrasonic additive manufacturing (UAM) techniques were used to simplify and miniaturize the ATA system by embedding the MPFL fluid channels directly into the integrated HX, CubeSat chassis, and the external radiator, creating integrated multi-function structures. The ATA system

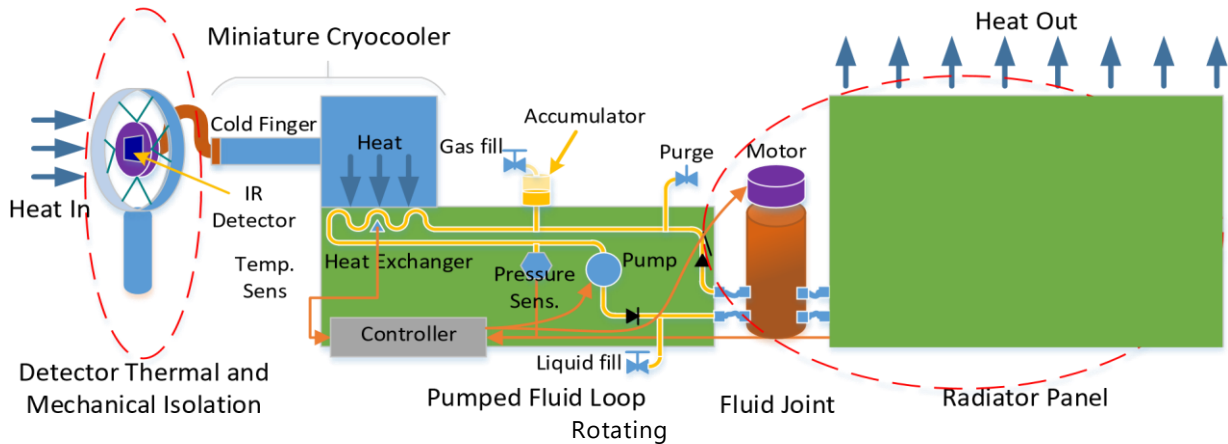


Figure 2-19: Conceptual operation of the ATA thermal control system. Credits: CSE/USU/ NASA/JPL.

also features flexible, multi-axis rotary fluid unions, and an integrated geared micro-motor which allows for the two-stage deployment and solar tracking of the ATA radiator. The ATA also features passive vibration isolation and jitter cancellation technologies such as a floating wire-rope isolator design, particle damping, flexible PGS thermal links and a custom Kevlar isolated cryogenic electro-optical detector mount. Next figure shows some of the technologies developed for ATA as well as the ground-based prototype CubeSat.

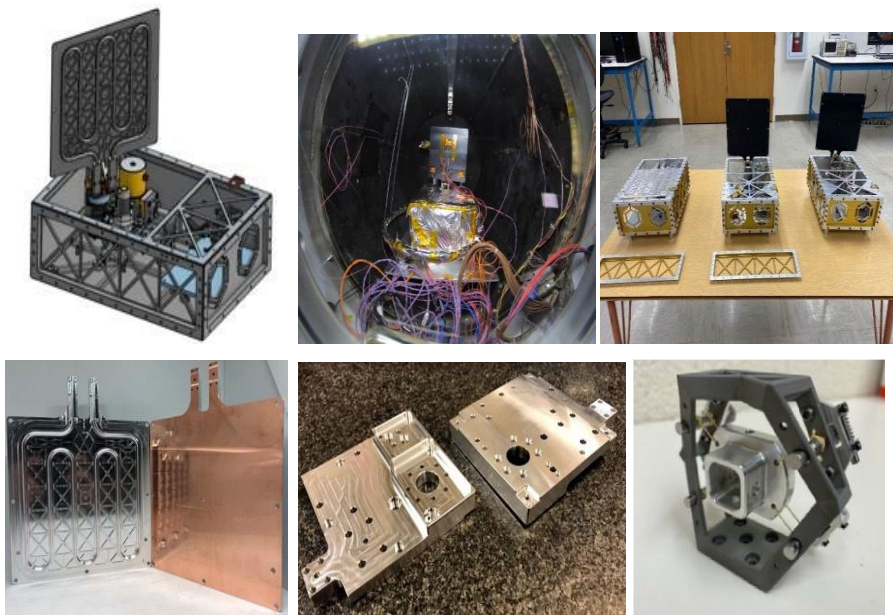


Figure 2-20: From top left: ATA CubeSat prototype, ATA subsystem testing, ATA prototypes, UAM radiator with copper backing, UAM heat exchanger, Kevlar isolated Cryogenic Electro-optical prototype mount. Credit: CSE/USU/NASA/JPL.

2.3. Thermal Control Summary

As thermal management on HAPS is limited by mass, surface area, volume and power constraints, traditional passive technologies, such as paints, coatings, tapes, MLI, and thermal straps, dominate

thermal design. Active technologies, such as thin flexible resistance heaters have also seen significant use in HAPS, including some with advanced closed-loop control. Many technologies that have to date only been integrated on larger HAPS are being designed, evaluated, and tested for small HAPS to meet the growing needs of HAPS developers as small satellites become more and more advanced. Deployable solar panels that have been used by many other HAPS are paving the way for thermal deployable components, while advanced deployable radiators and thermal storage units are still undergoing testing for small HAPS.

The design of the PODs on HAPS wings requires careful consideration of the environmental control system (ECS). Unlike manned aircraft, the PODs only contain equipment, so the ECS can be simplified to regulate temperature, humidity and pressure without providing oxygen. The main factors that affect the ECS are the radiation exposure, the heat dissipation of the equipment and the external temperature at different altitudes. To achieve optimal thermal management, we propose to isolate the PODs with high-quality insulation and install air inlets and outlets for direct cooling. The air will flow through a heat exchanger that will adjust the temperature of the equipment using a gel-based system. The gel will transfer heat to or from the outside air depending on the altitude. We do not anticipate the need for forced air circulation with fans, as natural convection should be sufficient. The ECS will also include sensors, ducts and thermal cables to monitor and control the temperature of the PODs. We expect that this solution will provide adequate cooling at low altitudes and heating at high altitudes, while avoiding the complications of high-speed airflow or vacuum conditions.

Technology in active thermal control systems has started expanding to accommodate volume and power restrictions of a smaller HAPS; cryocoolers are being designed to fit within 0.5U volume that will allow small HAPS to use optical sensors and imaging spectrometers.

3. Thermal analysis

Aerostats and airships are lighter-than-air aircraft which have received renewed interest in recent years for high altitude applications including surveillance, communications, and power-raising. The aerostat would float at approximately 6 km altitude where, it can receive over three times the annual energy of a ground-based system. The electrical power will be transmitted to the ground via the tether. The aerostat will need to keep a constant shape during its ascent and operation despite changes in atmospheric pressure as such a ballonnet will be used to maintain a constant pressure inside the aerostat. The temperature of the lifting gas will directly affect its pressure and the pressure differential between the contained gas and the external atmosphere defines the stress experienced by the aerostat envelope. In balloons, which are allowed to expand and contract or aerostats and airships with ballonnet systems in which the lifting gas can also expand or contract, the lifting gas temperature will also influence the buoyancy of the system. Thermal analysis can therefore be used to assess the feasibility of an aerostat or airship design.

Much work has been done on the thermal analysis of scientific balloons to aid in the design and flight profile prediction. Scientific balloons are typically made from flexible films and pressurised such that they expand until they reach their float altitude at which they are fully expanded, and the gas pressure is equal to the ambient air pressure. Airships and aerostats are instead required to

maintain their shape during ascent and as such are designed with ballonets which allow air to enter or exit the envelope in order to maintain the internal super-pressure in the face of changing atmospheric pressure.

This report describes a new thermal model for an aerostat or airship that builds on previously published models but extends them to include the effects of a ballonet used for gas pressure control. The model is then validated against experimental results of an airship.

The airship will confront a complicated thermal environment with complex heat fluxes and affected by the resulting absorbed heat loads, as depicted in next figure. The thermal environment of the airship mainly comprises direct solar radiation, atmosphere diffuse solar radiation, earth albedo solar radiation, atmosphere infrared radiation (IR), earth IR radiation, internal IR radiation, external convection heat transfer between the ambient air and air-ship envelope, the internal natural convection heat transfer between the inside hydrogen and airship envelope.

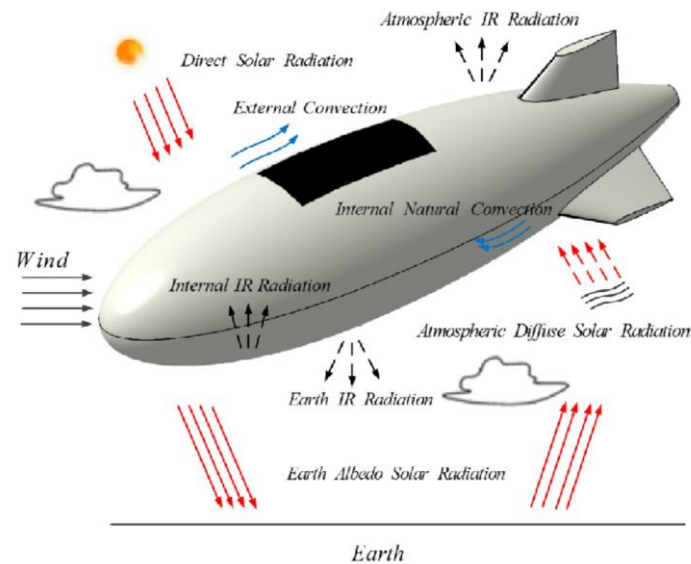


Figure 3-1: Thermal environment of stratospheric airship.

3.1. Photovoltaic (PV) array thermal model

The PV array was installed on the top part and center area of the airship hull, with a layer of heat insulation boards installed between the PV array and the envelope. The heat transfer mechanism of the PV array was described in next figure. The heat transfer of the PV array includes absorbed direct solar radiation heat flux $Q_{PV D}$, absorbed diffusive solar radiation heat flux $Q_{PV Atm}$ from atmosphere, external infrared radiation heat flux $Q_{PV IR Ex}$ to space, external convective heat transfer with outer atmosphere $Q_{PV Conv Ex}$, conductive heat transfer $Q_{PV Cond}$ to the envelope through the heat insulation layer beneath it, and the electrical power Q_{PVElec} converted from solar energy by the PV array, where R_e is the reflectivity of the earth surface.

3.2. Airship envelope thermal model

The general heat transfer mechanism of the airship envelope was portrayed in next figure. The heat transfer of the airship envelope include absorbed direct radiation heat flux Q_{EnD} from solar, absorbed diffusive solar radiation heat flux Q_{En_Atm} from atmosphere, absorbed albedo solar radiation heat flux Q_{En_Ear} from earth surface, external infrared radiation heat flux $Q_{En_IR_Ex}$ to space and earth surface, internal infrared radiation heat flux $Q_{En_IR_In}$ inside of the airship, conductive heat flux Q_{EnCond} through the heat insulation layer from the photovoltaic array, and the external convective heat transfer Q_{En_ConvEx} with outer atmosphere and internal convective heat transfer $Q_{EnConvIn}$ with Hydrogen.

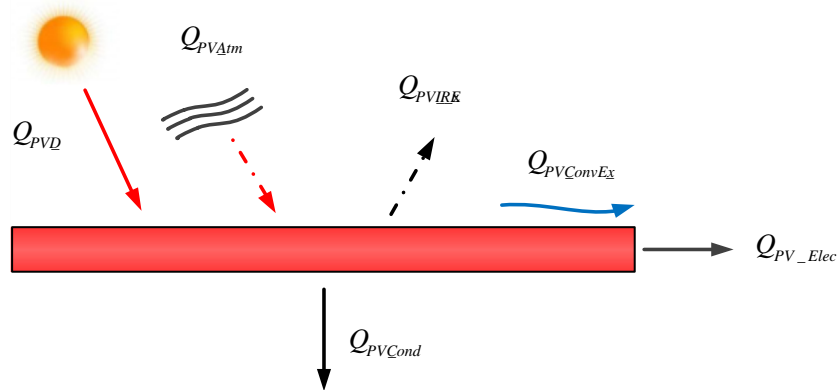


Figure 3-2: Heat transfer mechanism of PV

The actual heat load of the envelope varies with its location on the airship. The airship envelope beneath the PV array receives and emits no radiation flux and has no convective heat transfer with outer atmosphere. The airship envelope on the upper part of the airship that is uncovered by PV array has no heat transfer with earth surface, and no conductive heat transfer with PV array. The airship envelope on the lower part of the airship receives no direct solar radiation.

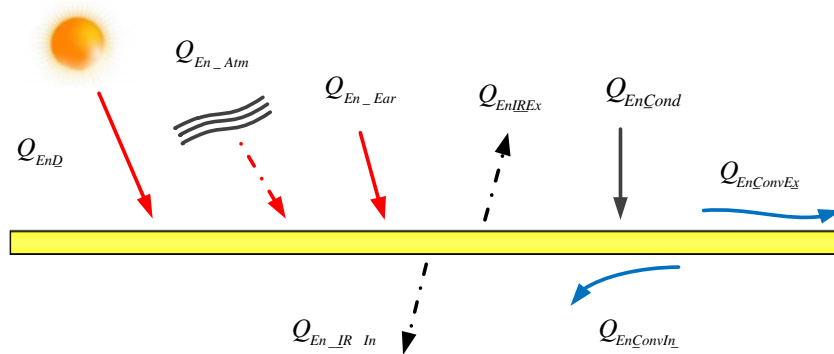


Figure 3-3: Heat transfer mechanism of airship envelope.

3.3. Hydrogen thermal model

The heat transfer mechanism of the internal hydrogen gas was depicted in next figure. The hydrogen was treated as radiation non-participating media, the heat transfer of hydrogen is internal natural convective heat transfer $Q_{He_Conv_In}$ with the airship envelope.

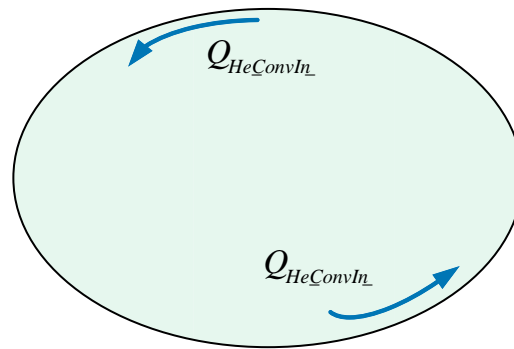


Figure 3-4: Heat transfer mechanism of Hydrogen.

3.4. Simulation methodology

The thickness of the PV array was about 5×10^{-4} - 1×10^{-3} m and airship envelope was about 1×10^{-4} - 2×10^{-4} m, so the PV array and airship envelope were treated as thin membrane. The thermal resistance along the normal direction of the membrane was neglected, furthermore, the conductive heat transfer on the other two orthogonal directions was neglected, given their low thermal conductivity and small cross area.

3.5. Governing equations

The numerical model is based on three dimensional Navier-Stokes equations, and control volume method was adopted in the CFD/Fluent simulation. The transient mass, momentum and energy governing equations which were necessary to investigate the temperature and flow field in the calculation domain were described as follows.

3.6. Solar Array

The solar array model uses the three-layer model of a cover glass, a photovoltaic cell array and a substrate. This model is shown in next figure.

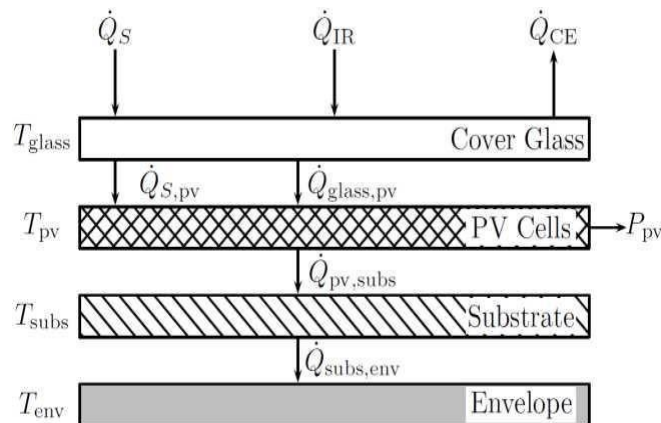


Figure 3-5: Solar array model

Glass is opaque to infra-red radiation and it is assumed that all the ground and sky IR radiation that is not absorbed by the glass is reflected. Therefore, there is no attenuated IR radiation falling on the photovoltaic cells.

3.6.1. Ballonet Membrane

As shown in next figure the membrane splits the internal volume of the airship into two parts. The upper surface of the membrane will be subject to radiative heat transfer with the upper elements of the envelope internal surface and convective heat transfer with the lifting gas. The lower surface of the membrane will exchange radiation with the lower elements of the envelope internal surface and have convection with the ballonet air.

3.6.2. Lifting Gas

The lifting gas will exchange heat with the airship envelope and the top surface of the ballonet membrane via convection: the heat flux to the lifting gas is the sum of the internal convection terms of all elements of the ballonet membrane on the lifting gas side and all envelope elements above the ballonet membrane.

3.6.3. Ballonet Air

Like the lifting gas, the ballonet air will exchange heat with its surroundings: the lower portion of the envelope and the lower surface of the membrane where the heat flux to the ballonet air is the set of envelope elements below the membrane.

3.6.4. Solar Radiation

There are three sources of solar radiation that will cause thermal loads on the airship: direct radiation from the Sun, diffuse radiation from direct radiation which has been scattered by the atmosphere and radiation reflected from the Earth's surface. These are designated and are calculated, along with the solar angle. The incident radiation on an element will be the sum of the three of these multiplied by their respective incidence angles.

Only the elements of the envelope that are not covered by the solar array will receive solar radiation along with all elements of the cover-glass. The radiation the solar cells receive will have been attenuated by the cover glass and so the absorbed incident radiation on an element of the solar cells where the absorptivity of the solar cells. Some of this absorbed radiation will be carried away in the form of electrical power.

3.6.5. Infrared Radiation

The airship will absorb infrared radiation from the ground and from the sky and emit infrared radiation. The envelope and solar arrays cover glass are assumed to be grey bodies where the absorptivity in the infrared range is equal to their emissivities.

In this model, the radiation from the ground and sky are given in the experimental results where the emissivity of the ground, values for which can be found in (4).

3.6.6. Internal Radiation

The envelope will radiate internally as well as externally. Hydrogen is transparent to infrared radiation and it is assumed that the air in the ballonnet is also, so all the internally emitted radiation must be absorbed or reflected by the envelope.

There are two meshes used for internal radiation calculations in this model, one for the lifting gas section that includes the envelope elements above the membrane and the membrane elements and the other for the ballonnet section which contains all the envelope elements below the membrane and the membrane elements is the sum of the infrared radiation emitted by element i and the incident radiation from other elements which is reflected by element i .

3.6.7. Conduction

In the solar array there will be conduction from one layer to another although conduction between elements of each layer is ignored in this analysis. The heat transfer between one layer and the adjacent layer is where the thickness and thermal conductivity of layer respectively. Conduction from the solar array substrate to the airship hull is considered but conduction from the outer layer to the inner layer of the envelope is not. This is because the envelope material is very thin so the temperature can be assumed to be constant throughout its cross-section. Additionally, no conduction over the surface of the envelope is considered due to the fact that each element will have a temperature very close to its neighbours and so the heat flux by conduction between elements will be very small in comparison to the heat fluxes already described. Previous studies use this approach to reduce the complexity (and thus computational time) of the simulation without much loss of accuracy.

3.7. Boundary conditions

3.7.1. Mass and momentum conservation equations

It was assumed that the airship was hermetic, so there is no mass exchange between the airship and the outer atmosphere. The airship envelope was treated as thin membrane where velocity was zero.

3.7.2. Energy conservation equations

Energy boundary conditions for PV array. For the PV array surface element i , S_T comprise the radiative, conductive, external convective heat flux, and the electricity power converted from absorbed solar energy, as was proposed in the PV array thermal model:

$$S_{T_PV_i} = \frac{1}{4} Q_{PV_D,i} + Q_{PV_Atm,i} + Q_{PV_IR_Ex,i} + Q_{PV_Cond,i} + Q_{PV_Conv_Ex,i} + Q_{PV_Elec,i}$$

The exact calculation of the above-mentioned heat sources were listed as follow. The absorbed direct solar radiation heat flux:

$$Q_{PV_D;i} = d_1 a_{PV} A_{PV;i} |d \cdot j_n s \cdot n_{PV}|$$

where a_{PV} is the solar absorptivity of the PV array, $A_{PV;i}$ is the area of the element, n_s is the solar irradiation unit vector, n_{PV} is the normal vector of the outer surface of the PV array. And d_1 is the index which considers the self-shadowing of the PV array from the direct solar radiation.

The absorbed atmospheric diffuse solar radiation heat flux:

$$Q_{PV_Atm;i} = a_{PV} A_{PV;i} I_{Atm}$$

The external infrared radiation heat flux from the atmosphere and earth to the PV array:

$$Q_{PV_IR\ Ex;i} = e_{PV} A_{PV;i} r [u_{PV;i} (T_{Ear}^4 - T_{PV;i}^4) + (1 - u_{PV;i}) (T_b^4 - T_{PV;i}^4)]$$

where e_{PV} is the emissivity of the PV array, r is the Stefan Boltzmann constant, $u_{PV;i}$ is the view factor from the PV array element to earth, T_{Ear} is the temperature of earth's surface in K, $T_{PV;i}$ is the temperature of PV array element in K, T_b is the sky equivalent temperature in K, which can be calculated from

$$T_b = 0.052 T_{Atm}^{1.5}$$

where T_{Atm} is the temperature of atmosphere.

The conductive heat flux through the heat insulation layer from the envelope beneath the PV array:

$$Q_{PV\ Cond;i} = k_{IN} \cdot (T_{En;i} - T_{PV;i}) / d_{IN} \cdot A_{PV;i}$$

d_{IN} where $T_{En;i}$ is the temperature of envelope, k_{IN} and d_{IN} are the thermal conductivity and thickness of heat insulation layer, respectively.

The external convective heat transfer with outer atmosphere

$$Q_{PV_Conv\ Ex;i} = h_{Ex} A_{PV;i} (T_{Atm} - T_{PV;i})$$

With the external heat transfer coefficient h_{Ex} calculated by:

$$h_{Ex} = (2 + 0.47 Re^{0.5} Pr^{1/3}_{air}) k_{air} / d \quad Re < 5 \times 10^5$$

$$h_{Ex} = (0.0262 Re^{0.8} - 615) Pr^{1/3}_{air} k_{air} / d \quad 5 \times 10^5 < Re < 6 \times 10^8$$

where Pr_{air} and k_{air} are the Prandtl number and thermal conductivity of air, respectively.

The electricity power converted from solar energy:

$$Q_{PV_Elec;i} = g_{PV} d_1 a_{PV} A_{PV;i} |d \cdot j_n s \cdot n_{PV}|$$

where g_{PV} is the electrical efficiency of the PV array.

Energy boundary conditions for airship envelope. For the airship envelope surface element j , S_T comprises the radiative, conductive, external and internal convective transfer heat flux, which served as boundary conditions, as was proposed in the airship envelope thermal model:

$$S_{T\text{En}j} = Q_{\text{En}Dj} + Q_{\text{En}Atmj} + Q_{\text{En}Earj} + Q_{\text{En}IR\text{Ex}j} + Q_{\text{En}IR\text{In}j} + Q_{\text{En}Condj} + Q_{\text{En}Conv\text{Ex}j} + Q_{\text{En}Conv\text{In}j}$$

The exact calculation of the above mentioned heat sources were listed as follow.

The absorbed direct solar radiation heat flux:

$$Q_{\text{En}Dj} = d_2 a_{\text{En}} A_{\text{En}j} I_D |j n_s \cdot n_{\text{En}j}|$$

where a_{En} is the solar absorptivity of the airship envelope, $A_{\text{En}j}$ is the area of the element, n_{En} is the normal vector of the outer surface of the airship envelope. And d_2 is the index which takes into account the self-shadowing of the airship envelope from the direct solar radiation, which is defined as:

$$d_2 = 1 \text{ if } n_s \cdot n_{\text{En}} < 0 \text{ or } 0 \text{ if } n_s \cdot n_{\text{En}} > 0$$

The absorbed atmospheric diffuse solar radiation heat flux:

$$Q_{\text{En}Atmj} = a_{\text{En}} A_{\text{En}j} I_{\text{Atm}}$$

The absorbed earth albedo solar radiation heat flux:

$$Q_{\text{En}Earj} = d_3 a_{\text{En}} A_{\text{En}j} I_{\text{Alb}} |j n_e \cdot n_{\text{En}j}|$$

Here, d_3 is the index which takes into account the selfshadowing of the airship envelope from the albedo solar irradiation:

$$d_3 = 1 \text{ if } n_e \cdot n_{\text{En}} < 0 \text{ or } 0 \text{ if } n_e \cdot n_{\text{En}} > 0$$

where n_e is the normal unit vector of the earth's surface. It is assumed that the curvature effect of the earth's surface in view is ignored and the surface is treated as an immense plane with the normal unit vector n_e towards upward.

The external infrared radiation heat flux from the atmosphere and earth to the envelope:

$$Q_{\text{En}IR\text{Ex}j} = e_{\text{En}} A_{\text{En}j} r \cdot [u_{\text{En}j} (T_{\text{Ear}}^4 - T_{\text{En}j}^4) + (1 - u_{\text{En}j})(T_b^4 - T_{\text{En}j}^4)]$$

where e_{En} is the emissivity of the airship envelope, $u_{\text{En}j}$ is the view factor from the envelope element to earth, $T_{\text{En}j}$ is the of temperature of envelope element in K.

The internal infrared radiation heat flux inside of the airship (4):

$$Q_{\text{En}IR\text{In}j} = A_{\text{En}j} \cdot (G_{\text{En}j} - J_{\text{En}j})$$

where $G_{\text{En}j}$ is the infrared radiation falling on element j , $J_{\text{En}j}$ is the infrared radiation away from element j .

The conductive heat flux through the heat insulation layer from the PV array:

$$Q_{En\ Cond,i} = k_{IN} \cdot (T_{PV,j} - T_{En,i}) / d_{IN} \cdot A_{En,i}$$

The external convective heat transfer with outer atmosphere:

$$Q_{En-Conv\ Ex,j} = h_{Ex} A_{En,j} (T_{Atm} - T_{En,j})$$

The internal convective heat transfer flux $Q_{En\ Conv\ Tn,j}$ with hydrogen was computed by solving the mass, momentum and energy conservation equations inside of the airship.

Energy boundary conditions for Hydrogen.

The radiative flux for hydrogen was set to be zero, and the internal natural convective heat transfer with the airship envelope was computed by solving the mass, momentum and energy conservation equations inside of the airship.

3.8. Solution method

Starting from a CAD model created by CATIA software, then the CFD software was employed to create the computational domain, and hexahedral meshes were generated to discretize the computational domain.

The ANSYS/FLUENT software was employed to solve transient mass, momentum and energy governing equations with the complementation of solar ray tracing algorithm and user's defined functions.

The solar ray tracing algorithm was employed to calculate the shadows of the hull on the fins. The solar ray tracing algorithm takes a beam that is modeled using the sun position vector and illumination parameters, and applies it to walls that has been specified, to performs a face-by-face shading analysis to determine well-defined shadows on all boundary faces and interior walls, then computes the heat flux on the boundary faces that results from the incident radiation.

The user's defined functions were employed to customize boundary conditions. The atmosphere diffuse solar radiation, the earth albedo solar radiation, atmosphere infrared radiation (IR), earth IR radiation, and external convection heat transfer coefficient between the ambient air and airship envelope, were implement by user's defined functions.

The coupled equations were solved by the Semi-Implicit Method for Pressure-Linked Equations (SIMPLE) algorithm which is based on pressure. For the convection term and diffusion term, the spatial discretization method was second order to provide efficient accuracy (ANSYS FLUENT 12.0 Theory Guide). The numerical simulation model of the experimental airship was described in next figure .

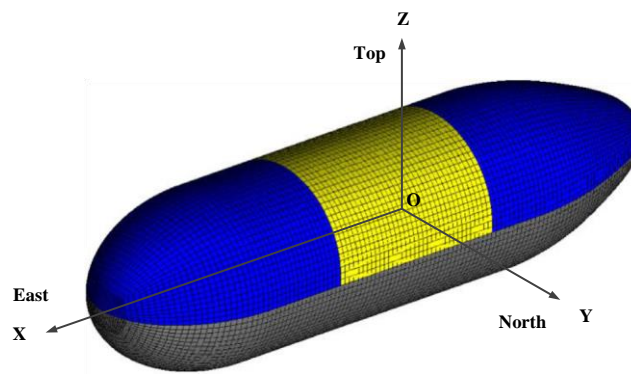


Figure 3-6: Hexahedral mesh and coordinate system of the experiment airship.

4. Results and discussion

After the validation of the thermal model proposed above, it was used to investigate the thermal performance of a stratospheric airship with PV array in stratospheric environment.

As the airship that used was without tail fin. To study the thermal performance of a stratospheric airship with photovoltaic array in the stratospheric environment, and investigate the influence of the airship tail fins, an airship model with typical configuration and tail fins was constructed for numerical simulation, which was different from that of the experimental airship.

The design index of the airship used for numerical simulation was shown in next table, the material thermal properties of the airship were shown in following table. PV array was installed on the center area of the upper part of airship hull, and a layer of heat insulation boards was installed between the PV arrays and the envelope. Three tail fins were placed uniformly on the back of the airship in inverted Y format with increment of 120. The fins were isolated from the airship main hull, so that the Hydrogen inside the fins could not circulate in and out.

Table 4-1: Design index of the airship.

Parameter	Value
Length, m	80
Volume, m ³	99,000
Diameter, m	20
Area, m ²	11,600
PV array area, m ²	580
PV array electrical efficiency	10%
Floating altitude, km	20

Table 4-2: Material thermal properties of the airship.

Parameter	Value
PV array absorptivity	0.90
PV array emissivity	0.90
Envelope absorptivity	0.20
Envelope emissivity	0.80
Insulation layer thermal conductivity, W/(m K)	0.02

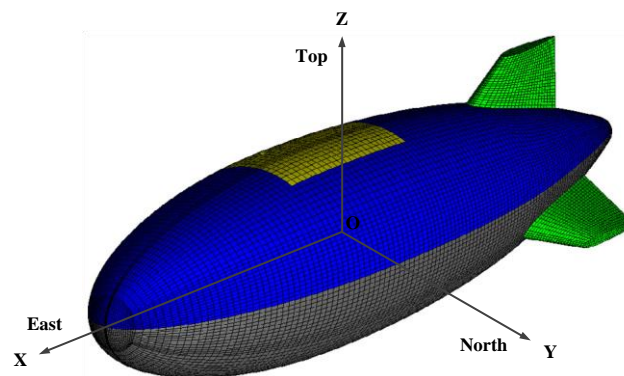


Figure 4-1: Hexahedral mesh and coordinate system of airship.

Previous figure represents the meshes and coordinate system used in this simulation. Assume that the airship was floating at 20 km. The differences in both maximum temperature and minimum temperature of the film were less than 1%.

The airship temperature characteristic was obtained by applying the method to the airship design index. Based on this, the Rayleigh number of the natural convection inside the airship was estimated to vary from 2.2×10^{10} to 6.2×10^{10} during the day and night cycle, indicating a turbulent flow regime. Therefore, the Realizable k-e turbulence model was used for this simulation, as described above.

4.1. Average temperature of airship surface

Next figure depicts the surface temperature history of the airship in 24 h. During the nighttime, the temperatures of the six parts of the airship are low and keep almost constant, ranging from 236.2 K to 245.6 K. As the upper part of the airship loss heat to the space through IR radiation while the lower part receive IR radiation heat form the earth surface, the temperature of the upper part of the airship is lower than that of the down part of the airship.

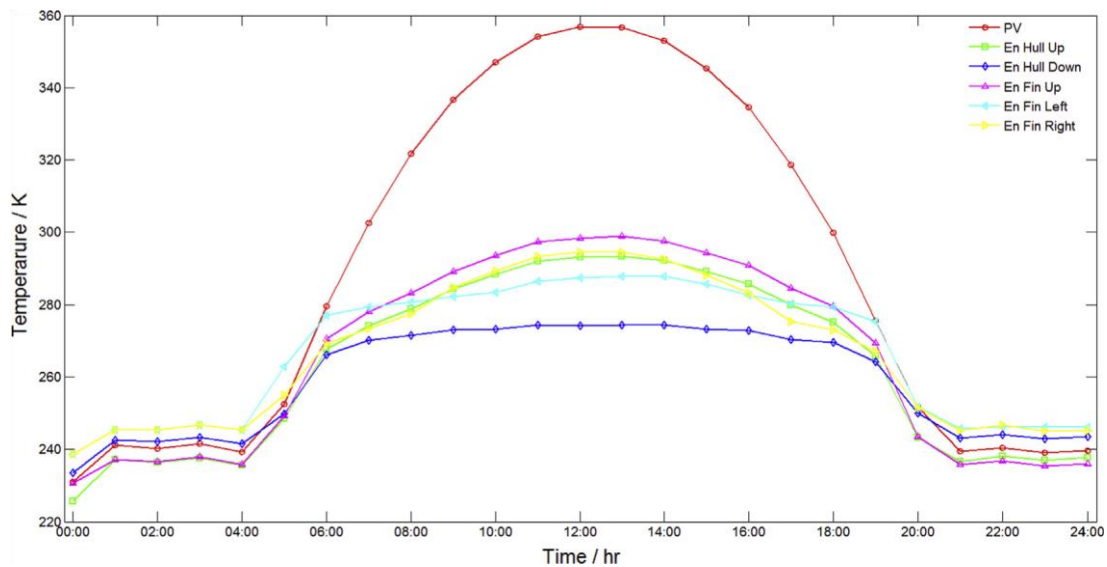


Figure 4-2: Average temperature of airship surface.

During the daytime, the temperature of the airship increase swiftly as the sun rise and reach its peak value at about 12:15 pm, then decrease to the steady state of the nighttime. At the time of 12:15 pm, the temperature of the PV array reached 356.8 K, the temperatures of the envelope at upper and down part of the airship hull are 293.1 K and 274.1 K, respectively.

The maximum surface temperatures of the up fin, left fin and right fin are 298.4 K, 287.4 K and 294.2 K, respectively.

As the sun position changes with time, the airship hull and up fin will shade the left fin and right fin from solar radiation, which would result in temperature difference among those three fins.

For the sun position in the sky, in the east and west direction, the sun is in the east from sunrise at 5 am to midday, then change to west until sunset at 20 pm. In the south and north direction, the sun is in the north from sunrise to 9 am, and change to south from 9 am to 16 pm, then return to north from 16 pm until sunset. In the altitude direction, the sun altitude increase from sunrise and reach its summit at midday, then decrease gradually until sunset.

The up fin was least shaded from solar radiation, so its temperature changes in the same trend with the PV, and its temperature was highest among the three fins at the midday.

The left fin receive solar radiation longer than the right fin, but was shaded by the hull and up fin at the midday. So its temperature rise early and decrease later than the up fin, with its temperature lowest among the three fins at the midday.

The right fin was shaded by the hull and up fin in the early morning and later afternoon but receives direct solar radiation at the midday. So its temperature rise later and decrease early than the up fin, with its temperature moderate among the three fins at the midday.

4.2. Temperature distribution on airship surface

Solar radiation and environment conditions change with time, which makes the surface temperature of the airship change correspondently. According to the relative position from the sun to the airship, the surface temperature distribution of the airship at 2 am, 6 am, 12 pm and 18 pm of the day were chosen to represent the four typical situations of nighttime, sunrise, midday and sunset, respectively.

Next figure (a)–(d) shows the temperature distribution of the airship at 2 am, 6 am, 12 pm and 18 pm of the day. To get a comprehensive understanding of the temperature distribution, each figure provides four perspective view of the airship, which are isometric view, side view, top view and bottom view.

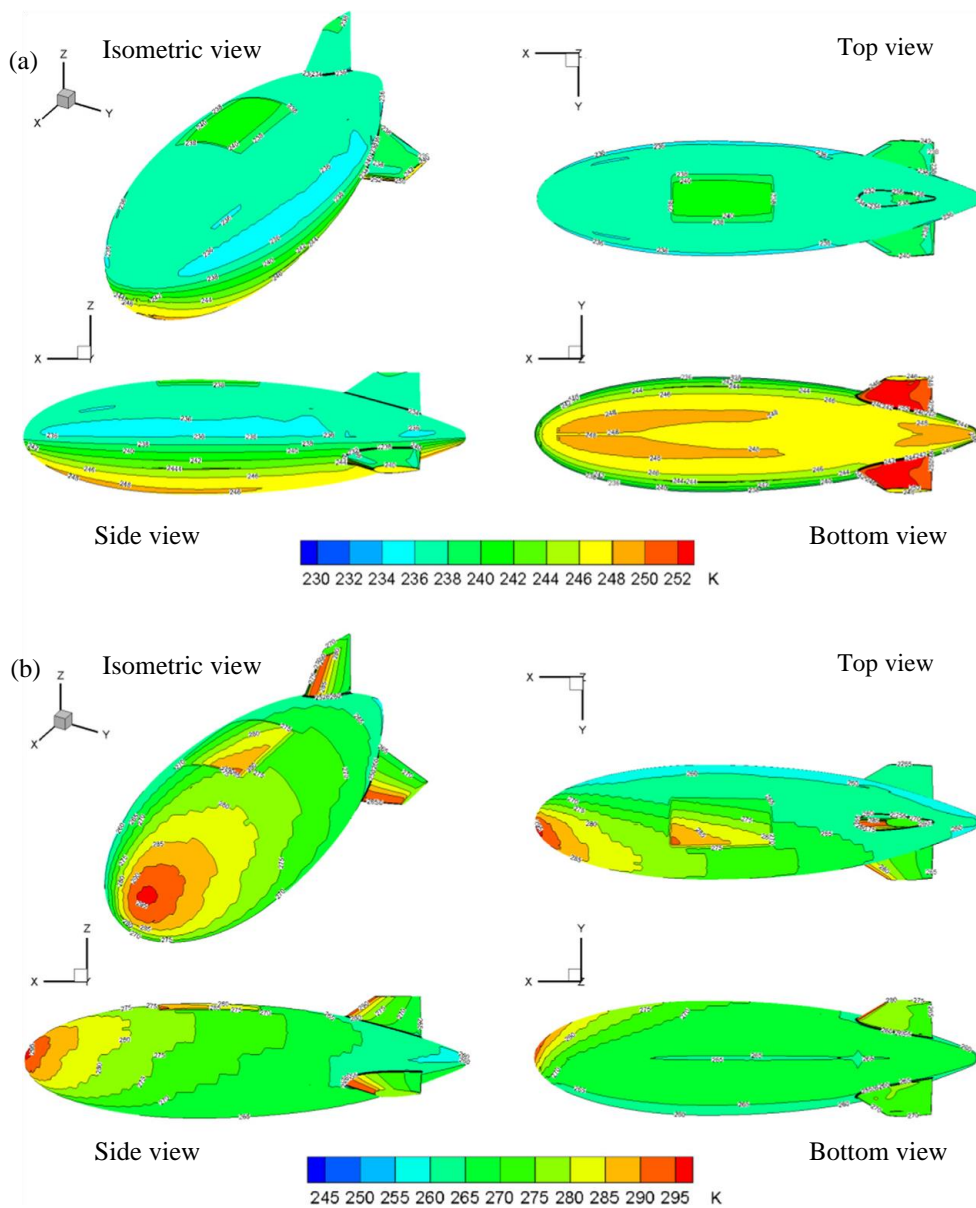


Figure 4-3: Temperature distribution on airship surface; (a) 2 am; (b) 6 am; (c) 12 pm; (d) 18 pm

At the nighttime of 2 am, there was no solar radiation figure (a) depicts that the high temperature area locates at the bottom of the airship and decrease gradually upward along the airship envelope. The maximum temperature at the bottom of hull and fin surface was 248 K and 252 K, respectively. The temperature of the upper envelope was low and distributed relatively uniformly.

At the sunrise of 6 am, solar radiation reached the airship from northeast figure (b) reveals that high temperature area locates at the front and northeast part of the hull, PV, up fin and left fin with the maximum value of 295 K, 290 K, 290 K and 285 K, while the right fin was shaded by the hull.

At the midday of 12 pm, the sun was high and on the south of the airship figure (c) reveals that the maximum temperature distributed at the upper part of the south area of the airship. The maximum temperature of PV reached 350 K, while the maximum temperature of envelope at the same position relative to the sun was 310 K. As part of the left fin was shaded by the hull and up fin, the temperature of left fin was relatively low.

At the sunset of 18 pm, while the sun was still above horizon and at the northwest of the airship figure (d) reveals that high temperature area locates at the back and northwest part of the hull, PV, up fin and left fin with the maximum value of 305 K, 310 K, 310 K and 310 K, while the right fin was partially shaded by the hull and up fin.

5. Conclusion

A numerical model was proposed to simulate the thermal performance of a stratospheric airship with photovoltaic array. A detail inspection into the temperature field and flow field distribution of the airship was conducted numerically. From the simulation results, the main conclusions were drawn:

- Solar radiation can exert great influence on the thermal performance of the airship. The temperature of the airship was low and keeps almost constant during the nighttime, ranging from 236.2 K to 245.6 K. And solar radiation can rise the temperature of the airship to the status ranging from 274.4 K to 356.5 K.
- The Hydrogen flow was strongly affected by temperature difference of airship surface, and the location of the maximum temperature area. The average velocity magnitude of Hydrogen inside the hull was about 0.5 m/s in the nighttime and 0.43 m/s during the daytime. The maximum velocity magnitude of Hydrogen inside the hull was about 1.4 m/s in the nighttime and can rise to 3.6 m/s at daytime.
- The higher temperature Hydrogen was gathered in the upper part inside of the airship, either heated by the bottom of the airship at nighttime or by the upper of the airship at daytime, and was forced to flow down, to form flow circles inside of the airship. The flow of Hydrogen was regular at nighttime but was rather chaotic in the middle and upper part of the airship at daytime.
- Affected by the shadow of hull and other fins, the temperature and velocity performance of fin was different from that of the hull and other fins.

Thermal analysis of airship, aerostat and scientific balloon designs aids in the assessment of their feasibility. In this report, a thermal model was developed for an airship that included a ballonet used to control the pressure of the lifting gas. The validity of this new model was demonstrated and shows a good agreement to previously published experimental data. The new thermal model presented in this report shows a stronger agreement with the experimental data than previously published models and as such can be used to provide a better analysis of future HAPS or airship designs that incorporate ballonet structures.

6. References

- (1) *Conceptual Design of an Energy System for High Altitude Airships Considering Thermal Effect*, Qiumin Dai 1,* , Daoming Xing 1, , Xiande Fang 2 and Yingjie Zhao 3,. (n.d.).
- (2) *Detailed Thermal Design and Control of an Observation Satellite in Low Earth Orbit*, Hilmi Sundu1,2,* , Nimeti Döner1, 1, Gazi University, Faculty of Engineering, Department of Mechanical Engineering, Maltepe, Ankara, Turkey 2. (n.d.).
- (3) *EFFECT OF ALTITUDE AND TEMPERATURE ON VOLUME CONTROL OF AN HYDROGEN AIRSHIP*, Prof. Antonio Dumas, Dr. Michele Trancossi Phd,, Dr. Mauro Madonia, Università di Modena e Reggio Emilia,. (n.d.).
- (4) *National Aeronautics and Space Administration, Chapter 7.-soa-thermal-2022*. (n.d.).
- (5) *THERMAL MODEL OF AN AIRSHIP WITH SOLAR ARRAYS AND A BALLONET*, D. Greenhalgh1, , A. R. Tatnall2, 1Faculty of Engineering and the Environment, University of Southampton, UK. (n.d.).
- (6) *Thermal performance of stratospheric airship with photovoltaic array*, Qiang Liu 1. , Yanchu Yang, Yanxiang Cui, Jingjing Cai, Academy of Opto-Electronics, Chinese Academy of Sciences, Beijing 100094, China. (n.d.).